Open Journal of Geology, 2023, 13, 847-882
https://www.scirp.org/journal/ojg
ISSN Online: 2161-7589
ISSN Print: 2161-7570

Hydrocarbon Prospectivity and Risk Assessment of "Bob" Field Central Swamp Depobelt, Onshore Niger Delta Basin, Nigeria

Charles Chibueze Ugbor, Celestine Ifeanyi Ugwuoke*, Peter O. Odong

Department of Geology, University of Nigeria, Nsukka, Nigeria
Email: *ifeanyi.ugwuoke.179089@unn.edu.ng

How to cite this paper: Ugbor, C.C., Ugwuoke, C.I. and Odong, P.O. (2023) Hydrocarbon Prospectivity and Risk Assessment of "Bob" Field Central Swamp Depobelt, Onshore Niger Delta Basin, Nigeria. *Open Journal of Geology*, **13**, 847-882.
https://doi.org/10.4236/ojg.2023.138038

Received: May 4, 2023
Accepted: August 21, 2023
Published: August 24, 2023

Abstract

This paper evaluates the hydrocarbon prospectivity and play risks of "Bob" field in Niger Delta Basin, Nigeria. The aim is to enhance exploration success through improved approach/technique by incorporating risk analysis that previous studies have not fully considered. This approach combines a set of analyses including stratigraphic/structural, amplitude, petrophysical parameter, volumetric and play risk using a suite of well logs and 3D seismic data. Maximum amplitude anomaly map extracted on the surfaces of delineated 3 reservoirs revealed 6 prospects, namely: Dippers, Cranes, Turacos, Nicators, Jacanas and Pelicans with hydrocarbon accumulation. Petrophysical analysis showed ranges of values for porosity, permeability and water saturation of 0.21 to 0.23, 158.96 to 882.39 mD, and 0.07 to 0.11, respectively. The various prospects yielded the following stock tank volumes 12.73, 6.84, 3.84, 11.32, 7.42 and 4.76 Million barrels (Mbls) each respectively in a column of 66 ft reservoir sand in the study area. Play risk analysis results gave: Pelicans and Nicators (low), Turacos and Dippers (moderate), while Jacanas and Cranes show high risk with minimal promise for good oil accumulation. The prospects possess good reservoir petrophysical properties with low to moderate risk, thus, viable for commercial hydrocarbon production, which increases confidence in management decisions for production.

Keywords

Seismic, Reservoir, Hydrocarbon Prospectivity, Risk Analysis, Volumetric, Niger Delta Basin

1. Introduction

Over the years, there has been a rapid increase in oil and gas exploration to meet rapidly increasing liquid fossil fuel energy demand worldwide. This has necessitated the application of sophisticated equipment and methods for its exploration to increase reserve. One of such steps is how best to understand the reservoir properties and architecture using a systematic approach in order to characterize and quantify the volume of hydrocarbon in place, and minimize prediction risks. For this reason, it becomes imperative to carry out formation evaluation to accurately determine the viability of the reservoirs within the "Bob" field in the Niger Delta Basin, Nigeria, and hence, ascertain the risks associated with the reservoirs. Hence, solving the different aspects of any problem with a view to obtaining a complete picture of the reservoirs in the study area through the integration of geophysical methods (such as geophysical well-log, seismic and production data) is the basis of this work. It is believed that such an integrated approach will allow for a more understanding of the subsurface under investigation and facilitate a precise mapping of the reservoir geometrics and its attendant properties and a better understanding of its lateral lithologic variation. Already, there are existing challenges in the study of hydrocarbon reservoirs using seismic and well data. An integrated approach is, therefore, advanced here to improve the reservoir resolution. Some of these challenges involve the reservoir architecture and trapping mechanism. For instance, it has also been observed that some thick reservoir sands do not necessarily contain economic accumulation of hydrocarbons compared with some thin reservoir sands with economic viability. This can be attributed to the trapping mechanism that is responsible for the accumulation. No single geophysical method or data set can completely be used to image and evaluate a reservoir completely and accurately, for instance, well-log or seismic data separately. This is because each method has its inherent limitation and ambiguities and so can only solve a certain aspect of a given problem. For instance, the seismic has a poor vertical resolution that makes detailed interpretation of the subsurface or recognition of reservoir heterogeneity at the reservoir scale difficult. On the other hand, the wireline logs do not give a good picture of the spatial organization within a reservoir. A method that combines the vertical and horizontal advantages of the 2 data sets becomes necessary to better depict the reservoir in 3 dimensions. Wiener *et al.* (1997) [1] carried out structural analysis in the Rifted Thrust Belt, Jianghan Basin, China using seismic and well-log data. They successfully interpreted the structural styles. El-Mowafy and Marfurt (2008) [2] used the Vertical Seismic Profiling (VSP) data to directly tie the seismic data to the geologic horizons. They realized structural and facies models that were consistent with the prevailing depositional processes, which showed that the faults were syn-depositional cutting across the younger horizons. Opara (2010) [3] carried out a prospectivity evaluation of an oil field in the Niger Delta, Nigeria from well-log and seismic data and delineated new prospects in the study area. Opara *et al.* (2011) [4] also studied an oil field in the Northern Depobelt using seismic and well-log data. They successfully delineated the structural styles in the area. Anyiam *et al.* (2017) [5] also utilized the integrated approach in their study of the field in the Niger Delta Basin. They proposed that for optimum reservoir production evaluation, it is necessary to ascertain appropriately the flow unit within the field using the integrated approach. Oyeyemi *et al.* (2018) [6] carried out hydrocarbon resource evaluation using combined petrophysical and seismic data analyses. They emphasized the success of the integrated approach in characterizing the hydrocarbon reservoir and identifying prospects in the field. They attributed the success of delineating the hydrocarbon prospects in the study area to the successful integration of the geological (well logs) and seismic data. Mode and Anyiam (2007) [7] worked on the reservoir characterization of Paradise Field. They concluded that the quality of the reservoirs is moderate to good and in some distal reservoirs, they are excellent. The average porosity values are approximately the same, but have variations in permeability that could be as a result of the compaction of the older reservoirs on the proximal part of the field. John and Oluwaseyi (2013) [8], in their petrophysical properties evaluation for reservoir characterization of "SEYI" field in the Niger Delta, reported that the reservoirs have good porosity and permeability to accumulate and yield a good quantity of hydrocarbon to wells. The present study is aimed at mapping the hydrocarbon prospects within the study area by integrating both seismic and well-log data through seismic data interpretation, petrophysical evaluation and play risk analysis using a more robust approach within the Petrel and Interactive Petrophysics software. The process includes establishing the reservoir sand distribution in the "Bob" field, determining the structural reservoir architecture, identifying the prospects, establishing the petrophysical parameters, calculating the quantity of hydrocarbon within the delineated reservoirs and prospects and carrying out the play risk assessments across the "Bob" field situated in the Central Swamp Depobelt of the Niger Delta Basin.

2. Geologic Setting of the Study Area

The Niger Delta Basin is an extensional rift basin that is located in the Gulf of Guinea and extends throughout the Niger Delta Province (**Figure 1**). It lies on the passive continental margin near the west coast of Nigeria. The delta has prograded southwestward from Eocene to Present, forming series of depobelts that represent the most active portion of the delta at each stage of its development [9].

These depobelts form one of the largest regressive deltas in the world with an area of about 300,000 km^2 [9]. The sediment has an average thickness of about 10 km in the centre of the depocentre and the estimated sediment volume is 500,000 km^3 [10]. The Niger Delta Basin has one petroleum system which was named as the Tertiary Niger Delta Petroleum System [9] [11]. This petroleum system originated at the RRR triple junction which began in the Late Jurassic and transited into the Cretaceous as a result of the opening of the southern Atlantic Ocean [12]. Ekweozor and Daukoru (1994) [11] and Tuttle *et al.* (1999) [12], reported that the basin started its development and piled up a thick sediment that is about 10 kilometers in the Eocene.

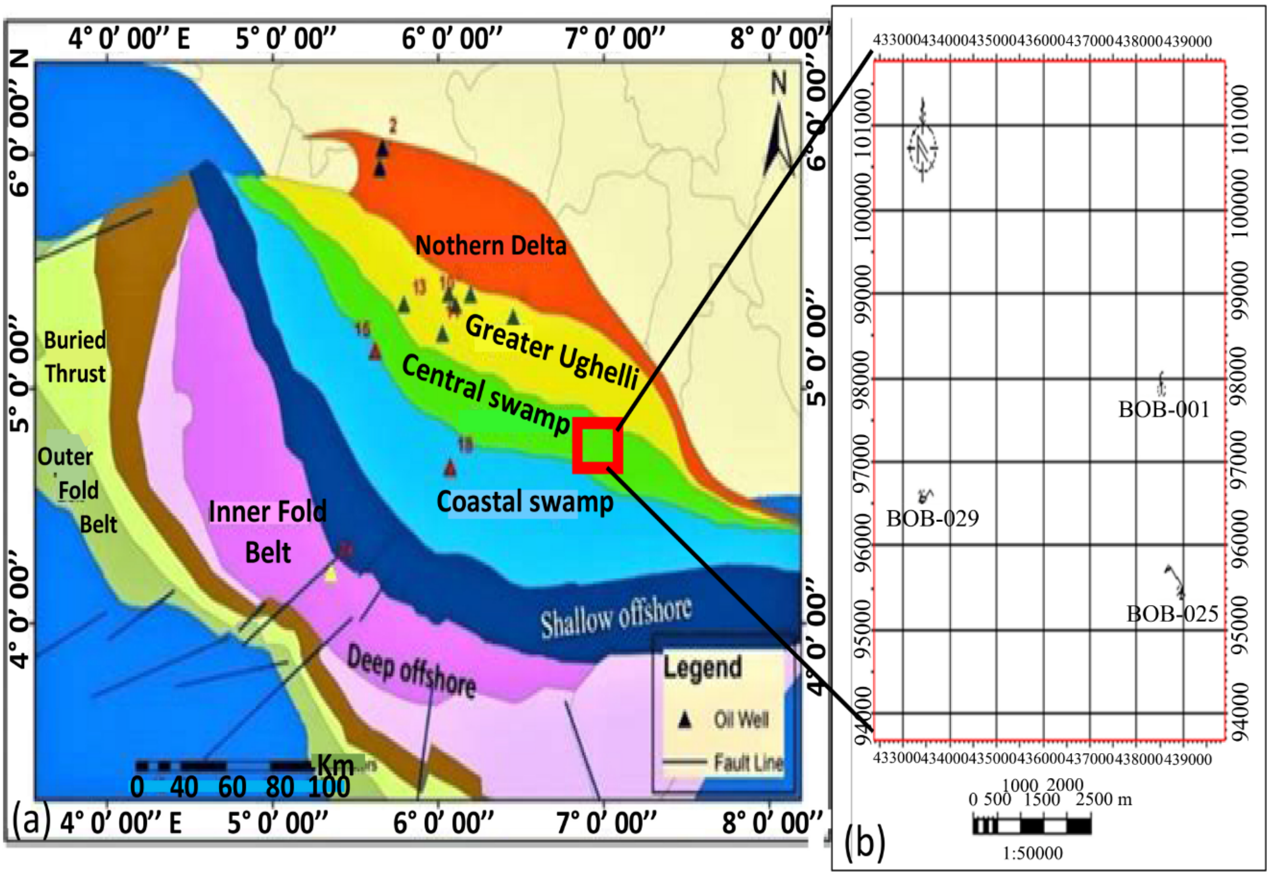

Figure 1. Location map of the study area in the Niger Delta Basin: (a) Inset map of Nigeria, showing the location of the Niger Delta, depobelts and the study area in the Central Swamp depobelt; (b) ***Base*** map of the study area showing the studied wells (modified from [13]).

The basin stratigraphy is divided into three formations; Akata, Agbada and the Benin Formations (**Figure 2**). The Akata Formation consists of shale formed during marine transgressive cycle and is the major source rock within the basin [12]. Agbada Formation is made up of predominantly sands deposited in essentially paralic environment. This constitutes the oil and gas reservoir within the basin. Ejedawe *et al.* (1984) [14], using the hydrocarbon maturation models, concluded that the shales of Agbada Formation contributed to the source rock in some parts of the Niger Delta. Similarly, after studying the source organic matter of shales of the Agbada Formation, Doust and Omatsola (1990) [13] concluded that the intraformational shales contributed to the hydrocarbon generation in the Niger Delta. Tuttle *et al.* (1999) [12] referred to Agbada Formation as the transition zone with intercalation of sand and shale. The Agbada Formation contains hydrocarbon traps that are mainly dip closures (rollover anticlines in growth faults) and few stratigraphic traps. The faults are essentially listric faults and form main barriers leading to compartmentalization of accumulated hydrocarbon. Benin Formation stratigraphycally occupies the topmost part of the Niger Delta and overlies the Agbada Formation. It consists of unconsolidated sands of about 2000 m thick [15] [16]. It is deposited in fluvial environment and

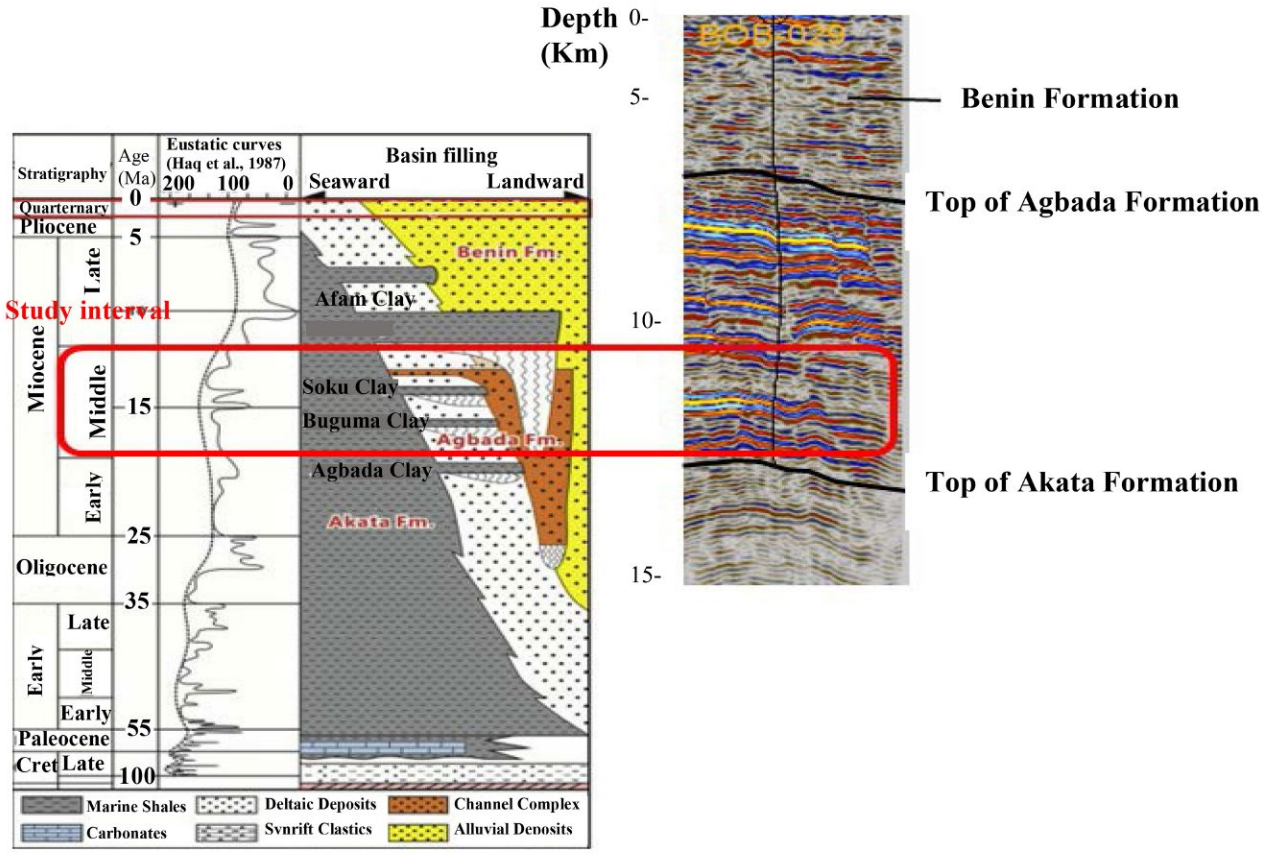

Figure 2. Niger Delta regional stratigraphy (modified from [17]) with appropriate location of the "Bob" field outlined in red in Agbada Formation in the Central Swamp Depobelt and correlated to the seismic section that penetrated the entire 3 formations of the delta.

made up of coastal plan sands. Doust and Omatsola (1990) [13] reported six depobelts in Niger Delta, which are distinguished primarily by their age. They are: Northern Delta (Late Eocene-Early Miocene), Greater Ughelli (Oligocene-Early Miocene), Central Swamp (Early-Middle Miocene), Central Swamp II (Middle Miocene), Coastal Swamp I and II (Middle Miocene) and Offshore (Pliocene). The "Bob" Field is located within the Central Swamp Depobelt in the Eastern Part of the Niger, Nigeria with three wells. The study area is situated within one of the concession blocks that lies in the Cross-River estuary bordering Cameroon. Figure 2 shows the stratigraphic section of the sediments of the Niger Delta basin, with a correlative panel fitting the study interval on the seismic covering most section of the basin.

3. Materials and Method of the Study

3.1. Materials

The materials available for this study include 3D seismic and checkshot data. Others are well logs such as Gamma Ray (GR), Sonic (DT), Density (DEN), Neutron (NEU), and Deep Resistivity (RES_DEEP). The software employed included the Schlumberger Petrel, and Interactive Petrophysics (IP). The 3D seismic is a pre-stack time migrated data. The Pre-stack, rather than Post-stack, seismic data was chosen because of the intended seismic attribute analysis which requires preserved original seismic attributes data available in pre-stack seismic data. Its positive peak polarity is red and negative trough polarity is blue.

3.2. Method

The study was carried out by running a set of analyses using the well and seismic data in the following order: Field wide reservoir correlation using well logs on Petrel Panel, Seismic data interpretation (faults and horizons) using petrel software, Prospectivity studies from seismic property analysis, Formation evaluation (petrophysical property analysis) using Interactive Petrophysics, Volumetric analysis, and Play risk analysis using Schlumberger Petrel software.

In the field-wide reservoir correlation using well logs on Petrel Panel, the well logs, GR, Den and Res were used to correlate and establish the trend, stacking pattern and lateral continuity of the reservoir and shale in the field using Petrel software. Three wells were used in the correlation. While the GR log was employed to establish the lithology (sandstone/shale packages), the resistivity log identified the hydrocarbon saturated columns. The density log consistency within the saturated column in the entire logs showed absence of gas.

The seismic data interpretation commenced first with a seismic to well match. This was to bring the seismic that was acquired in time to the same unit with the well log that were acquired in depth. The seismic data interpretation was carried out by both stratigraphic (horizon) interpretation and structural (fault) interpretation. Well tops were used to guide the appropriate choice of reflection loop on the seismic section. The procedure proceeded by advancing on the volume on an 8 grid interval until the entire volume was covered in a field wide interpretation. The established horizons and faults sticks were converted into surfaces and time structural maps were generated. These were dept-converted using the checkshot data. The resulting anticlinal structures became potential hydrocarbon prospects for further confirmation from seismic property interpretation subsequently. The surface area of the reservoir is also available from here to serve as input to the volumetric computation subsequently. The fault surfaces and pattern revealed the structural architecture of the field and the nature of reservoir compartmentalization. Potential new prospects were also established.

For the prospectivity studies from seismic property analysis 3 amplitude map data were generated to identify new prospects based on areas with booming amplitude anomalies. For this study, the Maximum amplitude, the root mean square amplitude and maximum energy were generated over the area using Petrel software. The booming amplitudes conformable with the structures as expressed by both contours and faults boundaries, in the area helped to identify new prospects that were further named.

Formation evaluation involved the determination of the petrophyscial parameters such as porosity, permeability, and water saturation for each of the identified prospects were obtained from the well logs using the Interactive Petrophysics software. The net to gross was determined from the well-log suits in Petrel software aligning with the identified prospects.

Seismic property interpretation involved seismic attribute analysis. This was targeted as direct hydrocarbon indicator using inbuilt tool within Petrel software. Three seismic amplitude attributes, namely, Maximum, root mean square and maximum energy were extracted over the surfaces of the potential prospects identified from the structural/stratigraphic seismic data interpretation. The amplitude anomaly maps were generated over the reservoirs of interest to evaluate the distribution and further confirm or establish the hydrocarbon prospects. The areas with booming amplitude and where the 3 different attributes are consistent are selected as prospects having characteristics direct hydrocarbon indicators. This was useful in the prospect delineation process.

For the volumetric analysis, the seismic data interpretation and formation evaluation output were input for volumetric analysis of identified prospects. Petrophysical parameters such as gross rock volume, net to gross (oil column thickness), water saturation, areal coverage of the prospect and formation volume factor were used to calculate the Stock Tank Oil Initially in Place (STOIIP) using the formula within Petrel software.

In the play risk analysis, 3 parameters, seal thickness, reservoir distribution and source depth (maturity) for each of the reservoirs were used to carry out the play risk of the reservoirs. For hydrocarbon to be found in an area, the three petroleum elements to be present aside from the right timing are source, reservoir and trap/seal have to be presence at the right time. Analyzing the distribution of each of these conditions will play a role in determining the possibility or otherwise of hydrocarbon accumulation. The purpose of this analysis is to further validate the hydrocarbon prediction from other studies such as from seismic data interpretation including structural, stratigraphic and seismic attribute analysis carried out in this study in terms of the confidence level or (safe) or risky the prediction is. The play risk analysis, therefore, tries to evaluate these three petroleum accumulation indicators to further assert the correctness of a prediction. The risks were classified into Low, moderate and high. The confidence of a reservoir having good chances of being a prospect diminishes with increasing degree of risk level. This is because the presence of high source depth (maturity), reservoir and seal/trap indicates high possibility (low risk) of hydrocarbon generation, accommodation space and entrapment, respectively. While the presence of low source depth (maturity), reservoir and seal/trap rock produces a reverse effect, *i.e.* low possibility (high risk). On the other hand when these petroleum elements are determined to be moderate in size, the possibility of hydrocarbon presence is ranked as moderate (moderate risk). The petroleum element status namely, high, moderate and low thus translates to low, moderate and high play risk, respectively. The contours of the risk element maps are, therefore, based on the status of the petroleum element in question. Thus contoured isopach maps of each of the three petroleum elements were generated and colour-coded as red, yellow and green represent high, medium and low contour values, respectively. These invariably also translate to high, moderate and low play risk, respectively. The interpretation of the play risk map is such that areas on the surface with high contour values represents low risk (and colour-coded red), areas that occupy moderate or medium portion of the map represents moderate (and colour-oded yellow) and areas that occupy low contour values represent high risk (and colour-coded green).

The Composite Risk Segment (CRS) map is a combination of the three play risk maps in one map. The CRS map thus comprises all play risk map of each of the three petroleum elements, source depth, reservoir and seal in one map. This, therefore, combines the colour-coded maps of seal thickness, reservoir distribution and source depth already generated during play risk analysis. The final composite map is generated by stacking of the contoured colour-coded maps from the three play risk maps in the order of colour dominance: red, yellow and green. In this case, red colour means that at least, one of the petroleum elements is lacking, hence within the areas represented by red, if any of the play risk segment maps showed red colour, then the composite map in that area is RED colour. If an area has no red, but combination of yellow and green, then the dominant colour in the composite map will be yellow. On the other hand, when all the play risk maps from the three elements are all green, then the colour of that area in the composite map will be GREEN (low risk). Thus the interpretation of the composite segment map is as follows: RED for high risk, YELLOW for moderate risk and GREEN for low play risk.

3.2.1. Fundamental Principles Employed in the Petrophysical Evaluation

In the petrophysical evaluation, the gross rock volume, porosity, volume of shale and water saturation were empirically determined. Some of the mathematical functions s employed are as follows:

Estimation of shale volume (V_{sh})

The volume of shale was calculated using Gamma Ray log. This was realized by calculating the Gamma ray log index first as can be seen in Equation (1):

$$I_{GR} = \frac{GR_{log} - GR_{min}}{GR_{max} - GR_{min}} \quad (1)$$

where, I_{GR} = Gamma ray index, GR_{log} = Gamma ray reading, GR_{min} = minimum gamma ray (clean sand), GR_{max} = maximum gamma ray (shale).

Volume of shale was finally calculated using the Larimov equation for tertiary deposits.

$$V_{sh} = 0.083\left(2^{3.7*I_{GR}} - 1.0\right) \text{ – (Tertiary unconsolidated sand)} \quad (2)$$

Estimation of porosity (Φ)

Wyllie's time average Equation (3) was used to estimate porosity from the sonic log [18]. In a poorly consolidated, unconsolidated and/or uncompacted reservoir sand, a correction factor is necessary. Equation (4) involving the empirical compaction factor was then applied to affect this correction.

$$\Phi_s = \frac{\Delta t_{log} - \Delta t_{mat}}{\Delta t_{fl} - \Delta t_{mat}} \quad (3)$$

$$\Phi_s = \left(\frac{\Delta t_{log} - \Delta t_{mat}}{\Delta t_{fl} - \Delta t_{mat}} * \frac{1}{C_p} \right) * 0.9 \quad (4)$$

Effective porosity was further calculated at each interval using the mathematical Equation (5):

$$\Phi_e = \Phi_s - \left\{ V_{sh} * \left(\frac{\Delta t_{sh} - \Delta t_{mat}}{\Delta t_{fl} - \Delta t_{mat}} \right) \right\} \quad (5)$$

where, Φ_e is the effective porosity, Φ_s is the sonic porosity, Δt_{mat} is the matrix interval transit time, Δt_{fl} is the apparent fluid interval transit time, Δt_{log} is the interval transit time from the sonic log, Δt_{sh} is the specific acoustic transit time in adjacent shales, V_{sh} is the volume of shale and C is the shale compaction coefficient.

Estimation of water saturation (S_w)

Water saturation was calculated using the Simandoux equation. This equation accounts for the effect of shale with regard to water saturation as given in Equation (6):

$$\frac{1}{R_t} = \frac{\Phi_e^m * S_w^n}{a * R_w} + \frac{V_{sh} * S_w}{R_{sh}} \quad (6)$$

where; V_{sh} is the volume of shale, Φ_e is the effective porosity, S_w is the water saturation of the uninvaded zone, R_t is the true formation resistivity, R_w is the resistivity of formation water, R_{sh} is the resistivity of shale, n is the saturation exponent, m is the cementation factor and a is the tortuosity factor.

Estimation of permeability (k)

Permeability is the property of a rock to transmit fluids. It is controlled by the size of the connecting passages (pore throats or capillaries) between pores. It is measured in Darcies or milliDarcies. The relation shown in Equation (7) was used to obtain permeability values for the reservoirs delineated [19].

$$K = 8581 * \frac{\Phi_e^{4.4}}{Swirr^2} \quad (7)$$

where; K is the Permeability in milliDarcies, Φ is the Porosity, $Swirr$ is the Irreducible water saturation.

3.2.2. Volumetric Analysis

The main fluid type of interest in the study area was oil based on the petrophysical analysis carried out and other criteria employed. It thus became imperative to estimate the quantity of oil within the reservoir. This was carried out by estimating the Stock Tank Oil Initially in Place (STOIIP). The total area of the delineated prospect in conjunction with the thickness of the reservoir and other petrophysical parameters were used in estimating the stock tank oil initially in place. The accuracy of volumetric estimation depends on reliability of porosity, fluid saturations, net-to-gross, gross rock volume and formation volume factor values. This estimation is very critical as the value determines whether or not production activities are feasible within the field.

$$\text{STOIIP} = \frac{\text{GRV} * \text{NTG} * \Phi * \text{Sh}}{\text{FVF}} \tag{8}$$

where; STOIIP = stock tank oil initially in place;

GRV = Gross Rock Volume (area of the prospect *x* thickness of the prospect);

N/G = Net-to-Gross;

Φ = Porosity;

Sh = Hydrocarbon Saturation;

FVF = Formation Volume Factor.

4. Result and Discussion

4.1. Result

4.1.1. Well Correlation

The Gamma Ray (GR), Density (DEN) and Resistivity (RT) logs were used to run a field-wide correlation in the Petrel software. **Figure 3** shows the correlation panel strapped to depth. The reservoirs and the intervening shales are correlatable across the 3 wells along the NW-SE. The well tops were used to constrain this interpretation further. The shales and the 3 reservoirs, R3, R4 and R5 are seen correlated across. The shaliness increases with depth. The resistivity and Density logs were used to identify the hydrocarbon bearing reservoirs as seen from the elevated values of resistivity in the identified sandstone columns. The non-deflection of the density log within the hydrocarbon saturated column indicates a homogenous hydrocarbon state, oil. The correlation panel shows that the reservoirs/sandstones are continuous across the field and the sandiness diminishes along NW-SE. It also showed that the shaliness increases with depth and the reservoirs are strapped top and bettom by well developed shale packages.

4.1.2. Stratigraphic Correlation of the Shales/Seals and Reservoirs Sand across the BOB 001, BOB 0025 and BOB 0029 Wells

The Gamma Ray (GR) log is a useful tool in characterizing a reservoir in terms of the stratigraphic architecture, distribution through correlation, understanding the depositional environment and sequence of the sediment packages. The Gamma ray log motifs have been used to discuss the brief stratigraphy of the reservoirs identified in the area, such as R5, R4, and R3 as shown in **Figure 3**. The depositional sequence is characterized by channel sand, tidally influenced channel sand, shoreface, and marine shale. In BOB 001 (**Figure 3**), below Reservoir 5 (R5) is made up of thick sequence of marine shale from 11830 to 1700 ft indicating a transgressive systems tract. Reservoir 5 consists of coarsening upward sandstone sequence, with abrupt termination at the depth of 11,675 ft. This is an evidence of regressive system. Reservoir 4 (R4) started at the base with a sharp increase of well sorted coarse grain sandstone at depth of 11,750 ft. This channel

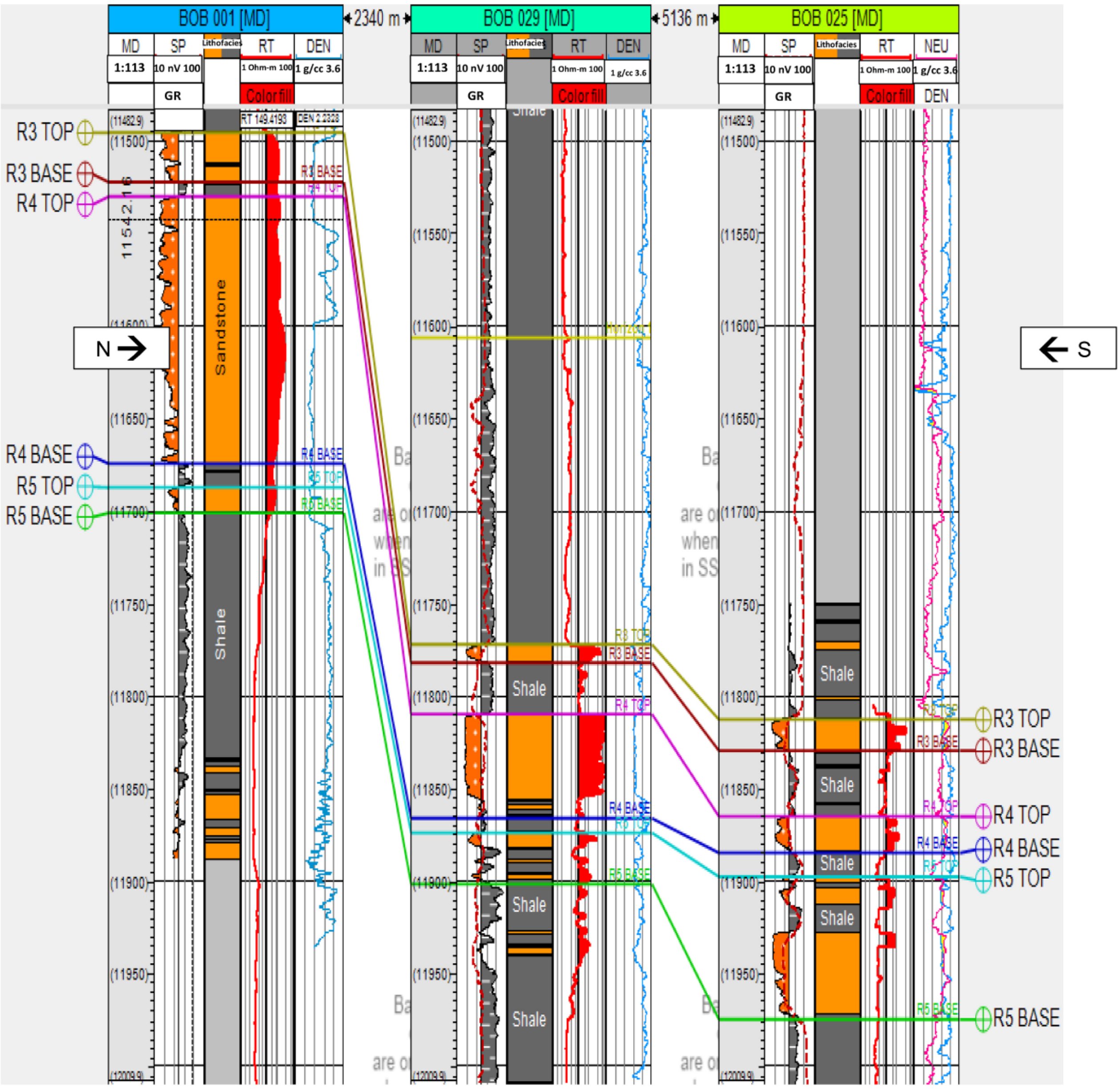

Figure 3. Correlation panel showing the distribution of the sandstone (reservoirs, R3, R4 and R5) and shale packages, across the wells in the study area, "Bob" field. The resistivity log peaks indicate zone saturated by oil.

sand continues up to 11,650 ft. This is followed by a short interval (11,650 - 11,645 ft) of sea level rise. A shallowing environment commenced from the 11,645 ft up to 11,620 ft. This is followed by a clean, well sorted sandstone between 11,620 and 11,530 ft. This is typical of channel sand, with characteristics blocky gamma ray signature. However this sandstone package is interbedded with a few intervals of clay lenses. This represents a tidally influenced high energy environment indicating interruption of the high energy by a brief lowering of low energy in a repeated cycle. Reservoir 4 (R4) terminates with a brief shallowing upward sequence which led to the deposition of the Lower shoreface sand. This is characterized by fining upward succession on top of the tidally influenced thick channel sand package. This is followed by a short interval of flooding surface starting from the 11,530 to 11,525 ft. This is made up of shale of relatively higher gamma ray. This is followed by a shallowing up sequence, leading to a coarsening upward sequence up to 11,515 ft depth. This sand package marks the base of reservoir R3 and represents an Upper shoreface. This basal portion of the reservoir is followed by a brief deepening marine incursion, which lead to the deposition of thin (about 5 ft thick) shale. The thin shale is too small to form a very strong baffle for intra reservoir fluid communication. The reservoir continues with a thick sequence of channel sand starting from a steep shallowing up sequence at the base. This is abruptly followed by a thick sequence of channel sand up to the top of the reservoir R3 at the depth of 11,495 ft. This indicates sedimentation in a low stand in essentially high energy environment. In wells BOB 029 and BOB 025, similar correlatable stratigraphic sequences are present. The reservoirs are underlain by varying thicknesses of marine shales, while the reservoir is channel sand deposits, with Upper and Lower shorefaces as described in the reservoir packages in BOB 001 well. The tidal influence in the channel sand reservoirs in the later wells are however less prominent than in well BOB 001. This indicates deposition in high energy environment with well sorted coarse grained sandstone in a Low Stand systems tract system in a shoreface delta.

Generally, there is increasing shaliness southwards and with increasing depth in all wells. The channel sand thickness decreased southwards, being highest at the Northernmost well (BOB 001) and least at the southernmost well, BOB 025. This is evidence in the thicknesses of all reservoirs (R3, R4 and R5) across the area. It is obvious that the sedimentation and the reservoir packages cut across the entire area as they essentially possess similar stratigraphic signature. They are dominated by the same channel sands, deposited in dominantly high energy environment, with intervening deepening of sea levels at intervals which resulted in deposits of shales in between. The overall coarsening upward sequence is replicated in all wells, showing that the energy level diminished seawards (southwards). Hence the sand packages is least at the southernmost part of the field (BOB 025) and highest towards the North (BOB 001). This implies that throughout the field, the sedimentation stated with high sea level rise in the deeper basin, while a receding sea level gave rise to deposition of coarser grained sands shorewise.

There is a reduction of sand thickness in reservoirs of well BOB 029. Reservoirs R3 and R5 are "hour glass" shaped, indicating a progressive transition from regressive to transgressive.

4.1.3. Seismic Data Interpretation

This includes stratigraphic, structural and property interpretation. The structural interpretation tries to identify the different reservoir sandstone packages from the seismic. The structural interpretation involves identifying the faults which hold the structural framework and trapping mecahnism in the reservoirs. The property interpretation is a further interpretation based on the seismic parameters to further characterize the reseroirs based on the variation of the chosen seismic parameter as direct hydrocarbon indicator. The first step in seismic data interpretation is to perform a well-to-seismic tie.

Well-to-seismic tie

The first stage in the structural interpretation of the 3D seismic data was a seismic-to-well tie. This was done to seamlessly combine the 2 data sets acquired in both time (seismic) and depth (well logs), by bringing them in the same unit. The primary data used for the seismic to well tie were density logs, checkshot and 3D seismic volume. Ancillary data are gamma ray logs and sand tops. Figure 4 is the seismic-to-well tie panel generated during the process. Figure 4 is a seismic to well tie showing reflection events on the seismic/synthetic seismogram corresponding to the mapped well tops for reservoirs (Res): R3 (red), R4 (red) and R5 (yellow) and the shales/seal/source tops (blue).

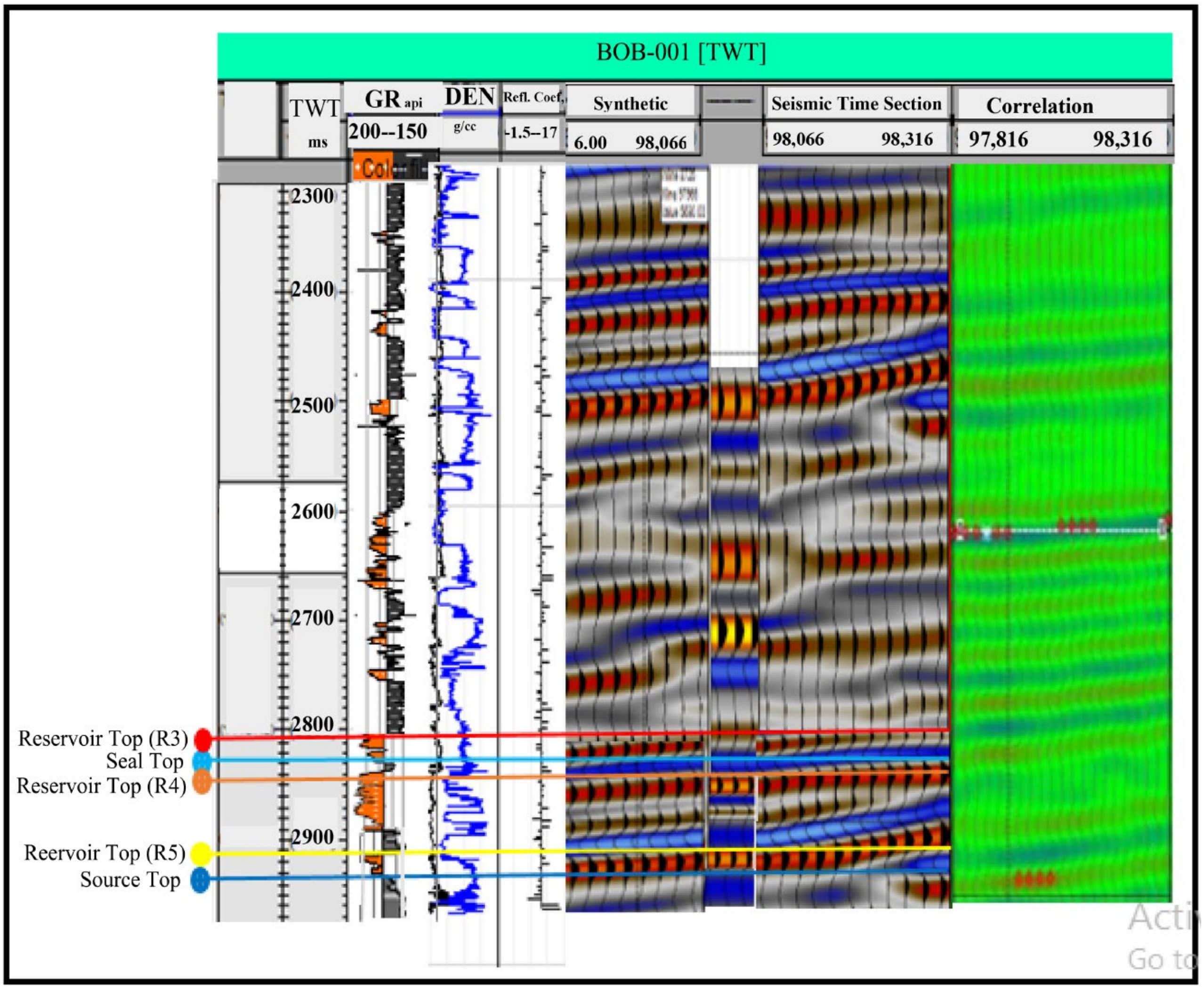

Figure 4. Seismic to well tie showing reflection events on the seismic/synthetic seismogram corresponding to the mapped well tops for reservoirs (Res.): R3 (red), R4 (red) and R5 (yellow) and the shales/seal/source tops (blue) generated by the authors during this study.

In this process, the reflection events identified on the seismic section on time domain was matched with the sand tops at corresponding depth on the well logs. Using the well logs, density and checkshot, a reflection coefficient was generated. This was convolved with a ricker seismic wavelet with zero phases from the seismic to yield the synthetic seismogram. Well tops and gamma ray logs were inserted to cross validate the established reflections on the seismic. A section of this log-derived (synthetic) seismogram was compared with the original seismic section to compare the correspondence of the reflection events in both seismograms. This match was good enough to progress with the seismic data interpretation. A good match was obtained in most of the horizons but at the deeper portions of the field where minimal bulk shifting for accurate tie was performed especially within the area of interest.

4.1.4. Horizon Interpretation

Horizons were mapped by picking along the cross line directions by following the intersection of the inline with the crosslines. The mapping interval was relatively kept constant, but some horizons were mapped at larger interval especially the regions with good reflection quality while some were mapped at closer interval in areas with poor reflection quality, marked by chaotic or irregular discontinuities in the reflection mass. This was carried out to minimize mis-ties to the barest minimum. A total of three horizons were mapped in the study area and named as H2, H3 and H4 corresponding to reservoirs R3, R4 and R5 across dip and strike sections. Additional tops mapped are H1 representing the seal top above reservoir R3 and the source at the base of reservoir R5. The strong **continuous** reflections of the horizons indicate that these stratigraphic surfaces are continuous across the field. **Figure 5** shows the interpreted horizons guided by the sand tops. The horizon was converted from time to depth using a polynomial velocity function built from the time-depth relation from checkshot data. The horizon tops, seal tops and source top from Well Bob 001 are shown as small white boxes. These tops can be seen in the well-to-seismic tie panel in **Figure 4**. The horizons picked are shown in **Figure 5(a)**. These horizons are also shown in 3D in **Figure 5(b)**.

The surfaces were established using input from the seismic to well tie, the sand tops and the gamma ray logs. The gamma ray log/sand top assisted in locating the reservoir top on the seismic prior to stratigraphic (horizon picking) interpretation in the seismic using the Petrel software. This also helped in establishing the seismic polarity colour on the seismic volume.

4.1.5. Fault Interpretation

Fault interpretation was carried out on every 10th grid along the inline direction; several faults were picked in the study area. One major Regional Fault (FR) was identified across the field extending nearly from top to the entire vertical section of the seismic. Also, seismic interpretation within the field revealed that the structural styles that characterize the field were mainly, apart from the one regional fault, are a few synthetic and antithetic faults (**Figure 6(a)**). These structures were consistent with the structural styles existing in the Niger Delta oil province as discussed by The presence of these faults in the study area is an indication that there is a possibility of hydrocarbon accumulation. The faults trend in a NW-SE direction and dip in a SW/SE direction. Fault sticks were generated from where fault polygons were created in the structure maps. **Figure 6(b)** shows the fault sticks generated from the structural interpretation.

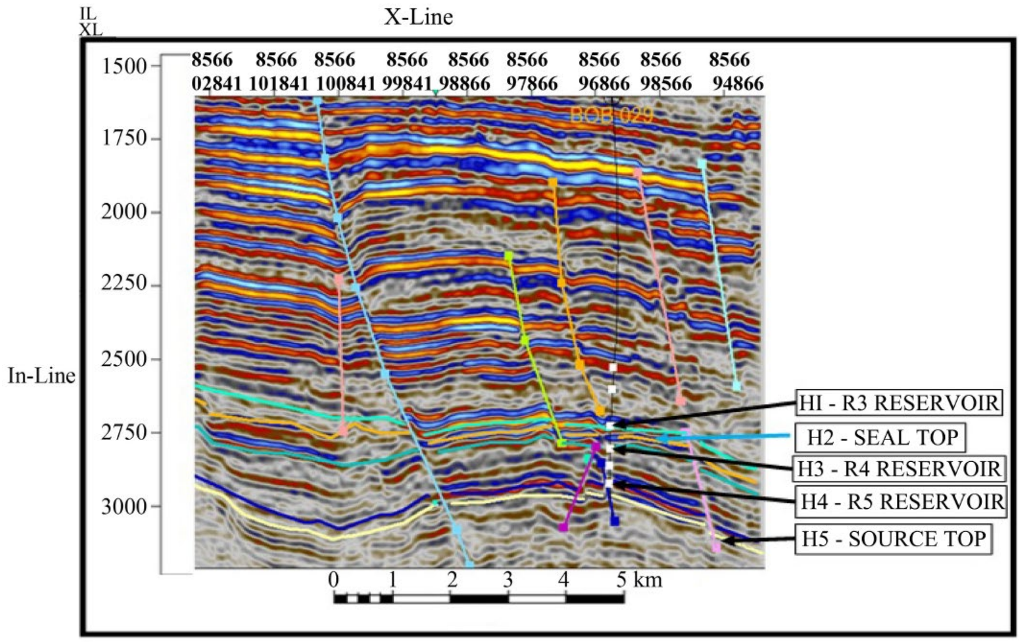

(a)

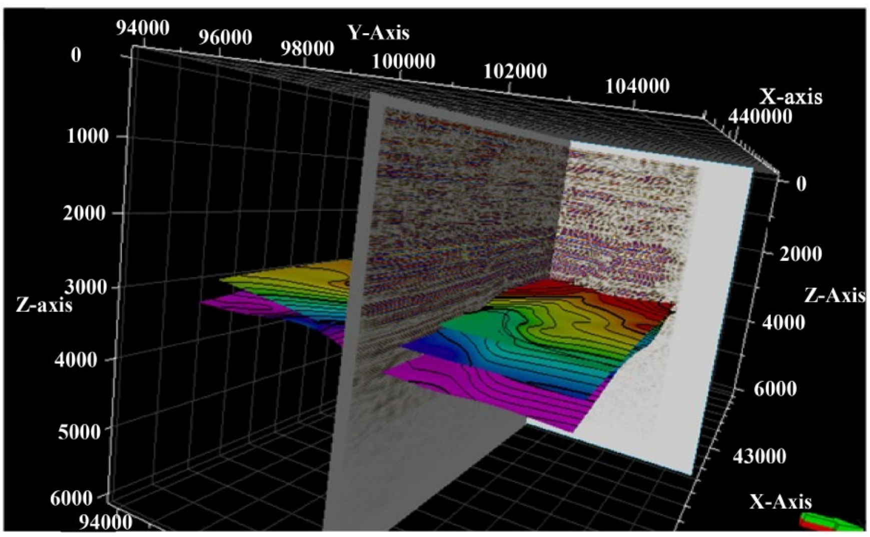

(b)

Figure 5. (a) Seismic section showing the interpreted horizons and the sand tops for the reservoirs. (b) Seismic time sections showing (a) mapped 3 horizons (H2, H3 and H4), (b) 3D volume map view showing time structure map of the 3 mapped horizons taken from 2810, 2845 and 9010 ms (twt), respectively (generated by the authors during this study).

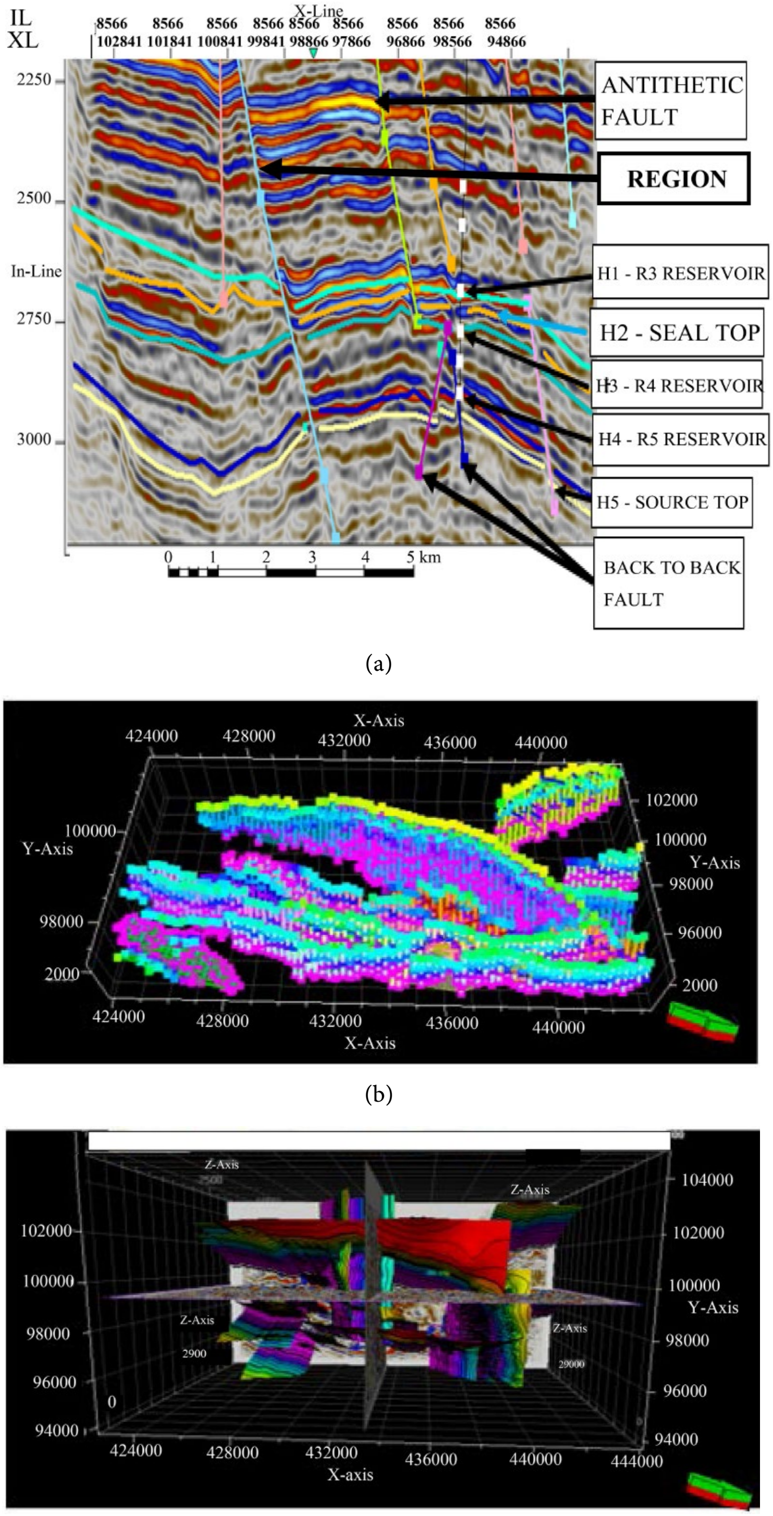

Figure 6. Seismic section (inline) showing the interpreted horizons and structures of (a) back to back faults, Regional Growth Fault (RF), Sythetic Fault (SF) and Antithetic Fault (AF). (b) Fault sticks from the structural interpreation showing esentially listric faults, 2-way and 3-way closures in 3D view. (c) Fault polygon visualization showing the distribution of the faults and horizons in 3D view (generated by authors during this study).

4.2. Structural Data Analysis

4.2.1. Fault Analysis from Seismic Data Interpretation

Different structural configurations were observed within the "Bob" field from the fault distribution and orientation. These structures such as back to back fault, regional fault with associated synthetic and antithetic faults serve as a flow barrier for hydrocarbon accumulation. The orientation of the observed fault within the "Bob" field was dominantly Northeast-Southwest trending (**Figures 7-9**). The delineated prospects were observed to be fault dependent closures capable of entrapping a reasonable quantity of hydrocarbon within the available reservoir compartments. The fault system is dominated by 2-way and 3-way fault closures as shown in **Figures 7-9**. These faults show evidence of structural control on the three reservoirs, R3, R4 and R5 is shown in the said figures. The time structure maps show fault surfaces generated from faults interpreted during the structural seismic data interpretation. For each figure, (a) represents the time structural map and the (b) represents the depth converted map. The closeness of each pair shows that the depth conversion was accurate.

Figures 7-9 are structural time/depth surface maps of the interpreted horizons and reservoirs showing the surfaces (horizon) and the faults. The contours show clear anticlinal structure as evidenced from the range of contour values which are lowest at the flanks (blue colour) and increasing to yellow and red portions (crest of each of the anticlines). The existing wells (Bob-001-003), mainly lie at the crest of the anticlines, a cross section taken across each of the structural maps could reveal this anticlinal form. The faults demarcate the reservoirs with the wells, Bob-03 and Bob-01 lying in different fault blocks. The fault surfaces are the thick black rigid bold faced curved surfaces running the surface of the map (across the contour lines in essentially NW-SE direction) are fault surfaces created from the fault sticks from the structural seismic data interrelation (**Figure 6(c)**).

4.2.2. Fault Analysis

Different structural configurations were observed within the "Bob" field from the fault distribution and orientation. These structures such as back to back fault, regional growth fault with associated synthetic and antithetic faults serve as flow barriers for hydrocarbon accumulation. The orientation of the observed fault within the "Bob" field was dominantly Northeast-Southwest trending (**Figures 10-12**). The delineated prospects were observed to be fault dependent closures capable of entrapping a reasonable quantity of hydrocarbon within the available reservoir compartments. The fault system is dominated by 2-way fault closures, though some 3-way fault closures are present.

4.3. Seismic Property Interpretation

Seismic amplitude attribute maps generated from the horizons showed that the fault closures are characterised by high amplitudes. Three wave amplitude properties, maximum, Root Mean Square (RMS) amplitude and average energy showed

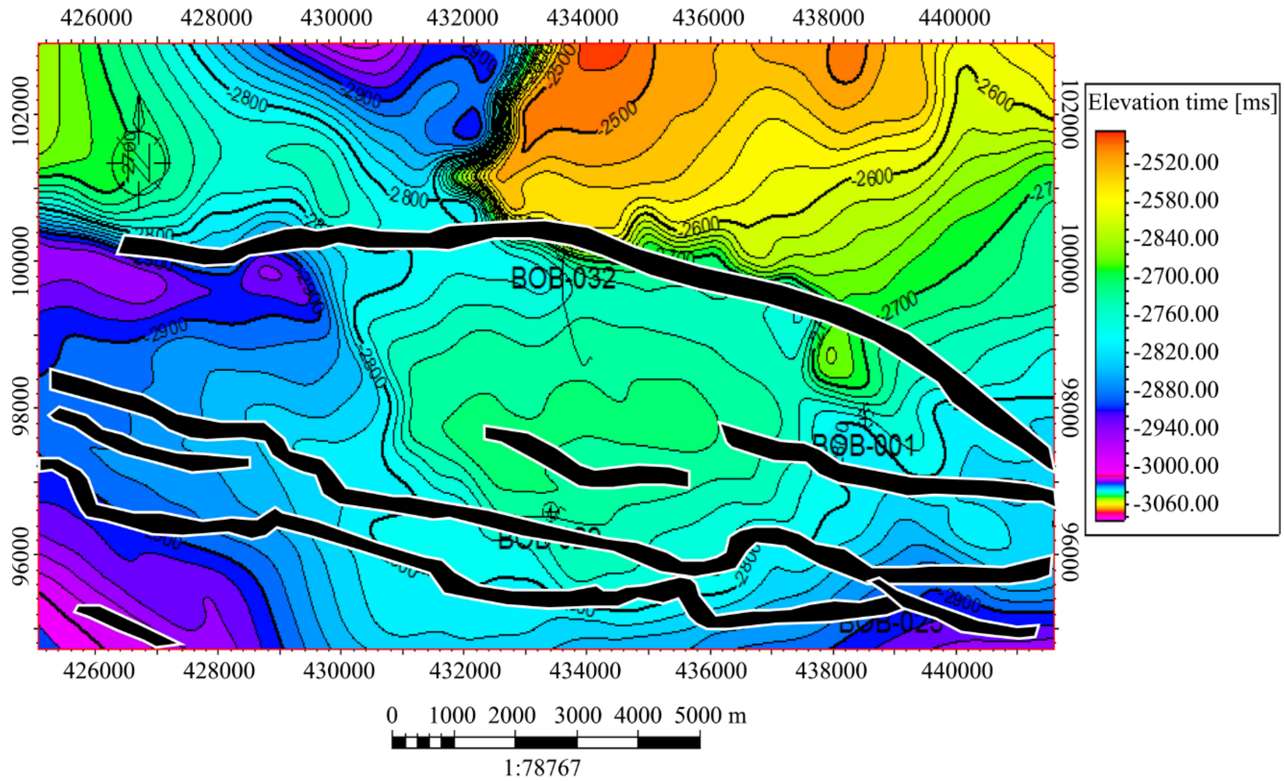

(a)

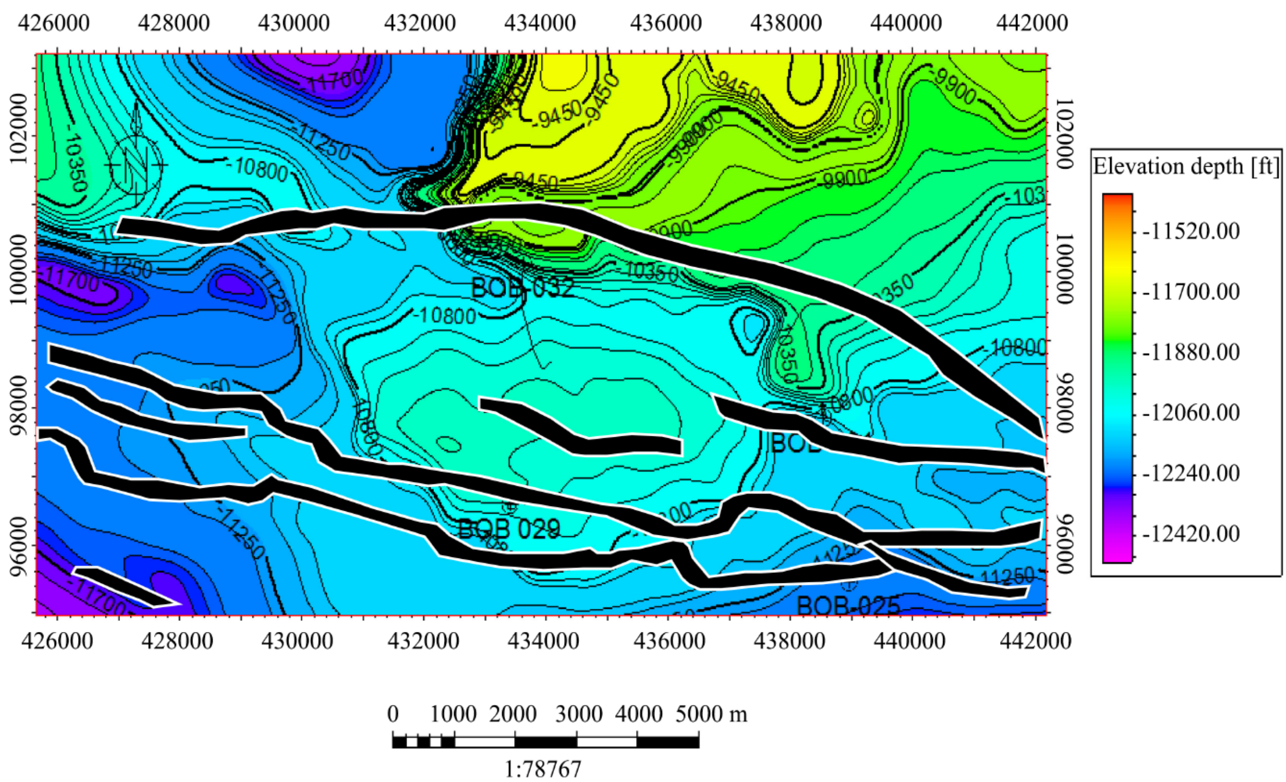

(b)

Figure 7. (a) Structural time map of H1 horizon (R3 reservoir); (b) Structural depth map of H1 horizon (R3 reservoir) (generated by the authors during this study).

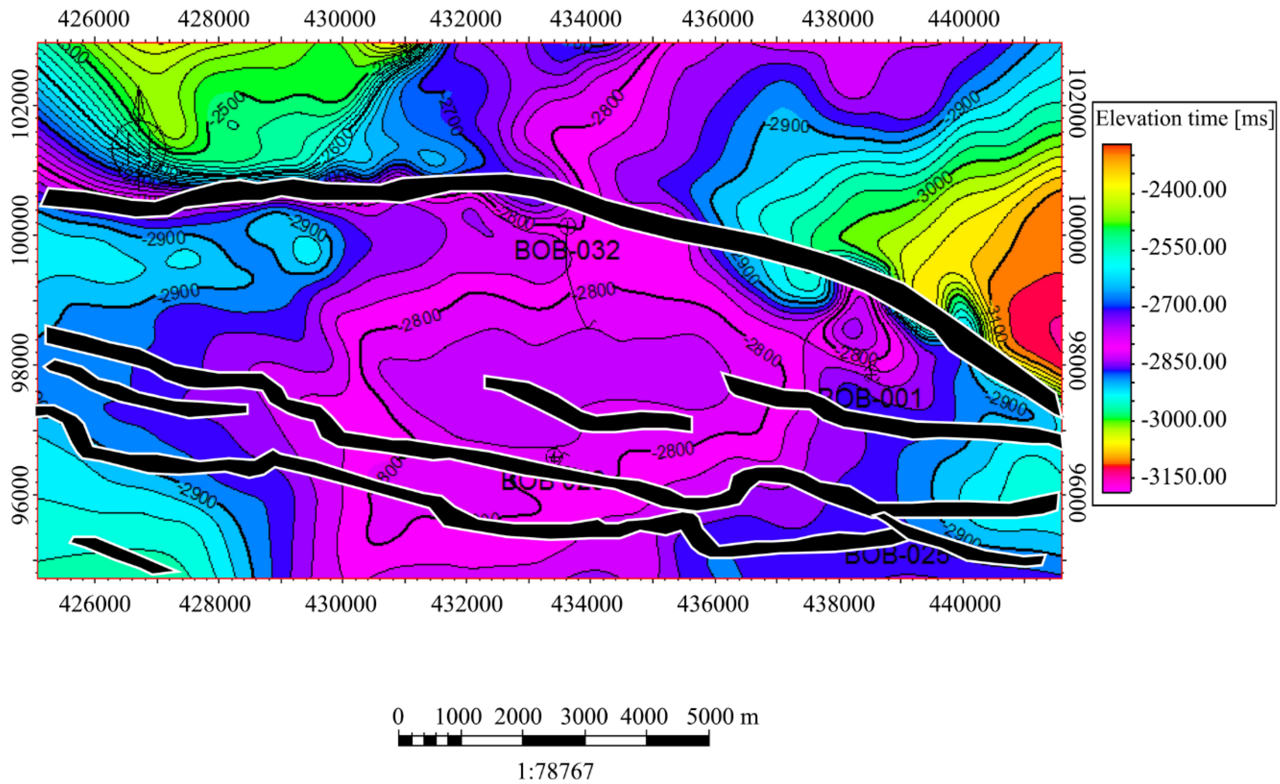

(a)

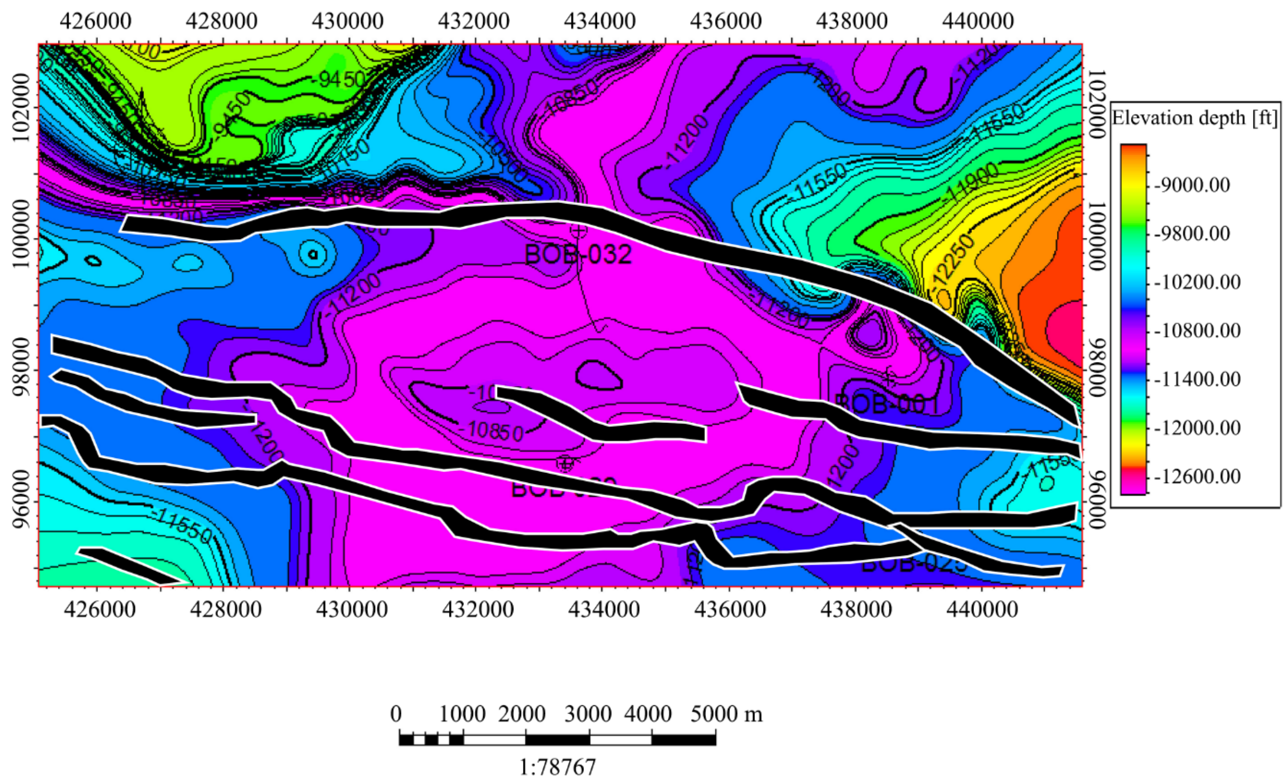

(b)

Figure 8. (a) Structural time map of H3 horizon (R4 reservoir); (b) Structural depth map of H3 horizon (R4 reservoir) (generated by the authors during this study).

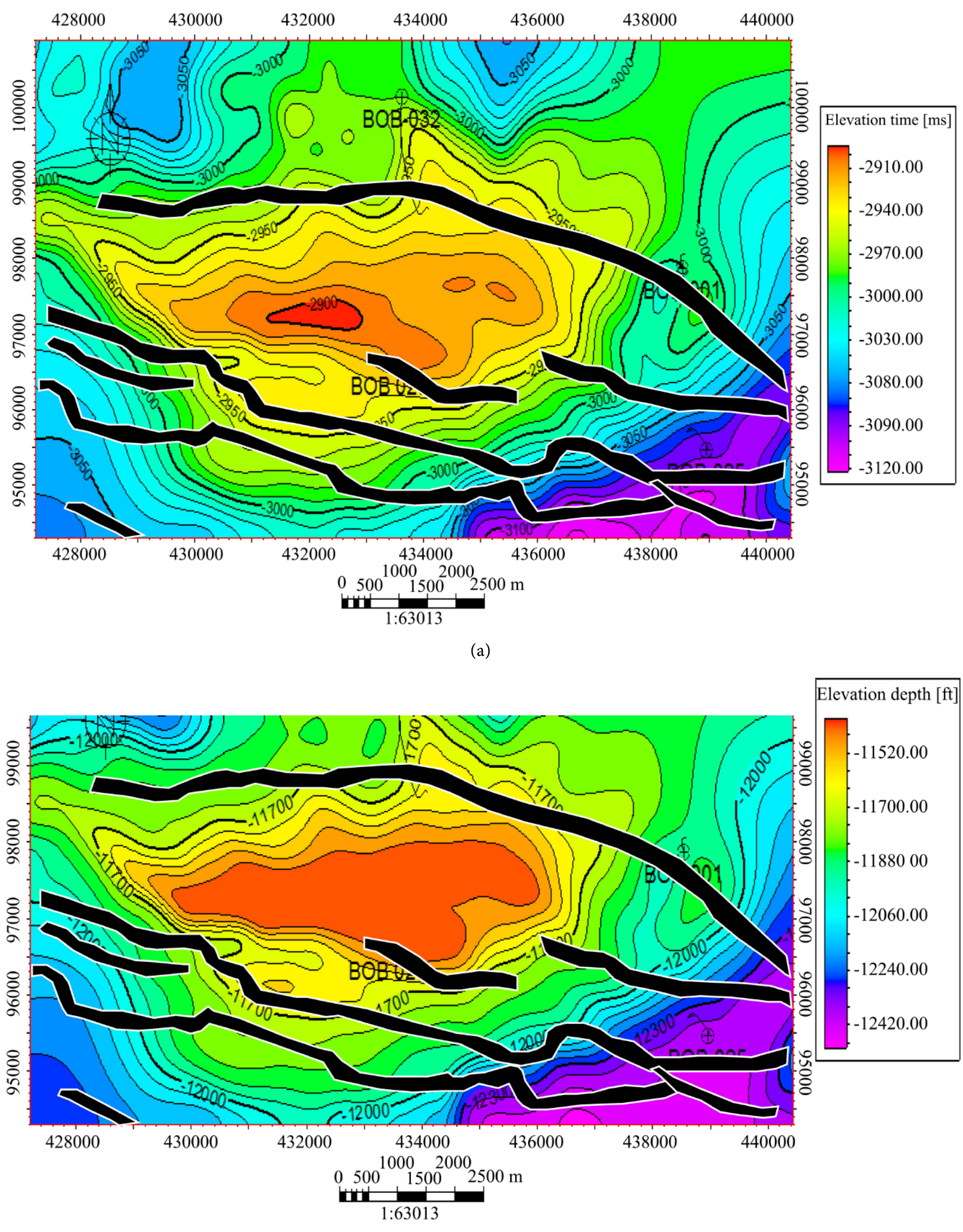

(a)

(b)

Figure 9. (a) Structural time map of H4 horizon (R5 reservoir); (b) Structural depth map of H4 horizon (R5 reservoir) (generated by the authors during this study).

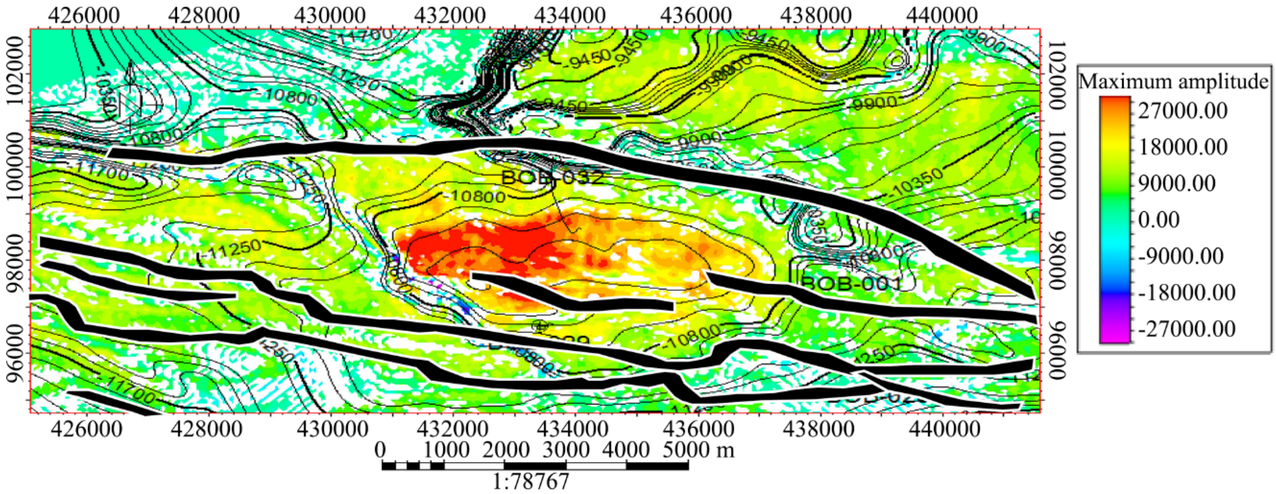

(a)

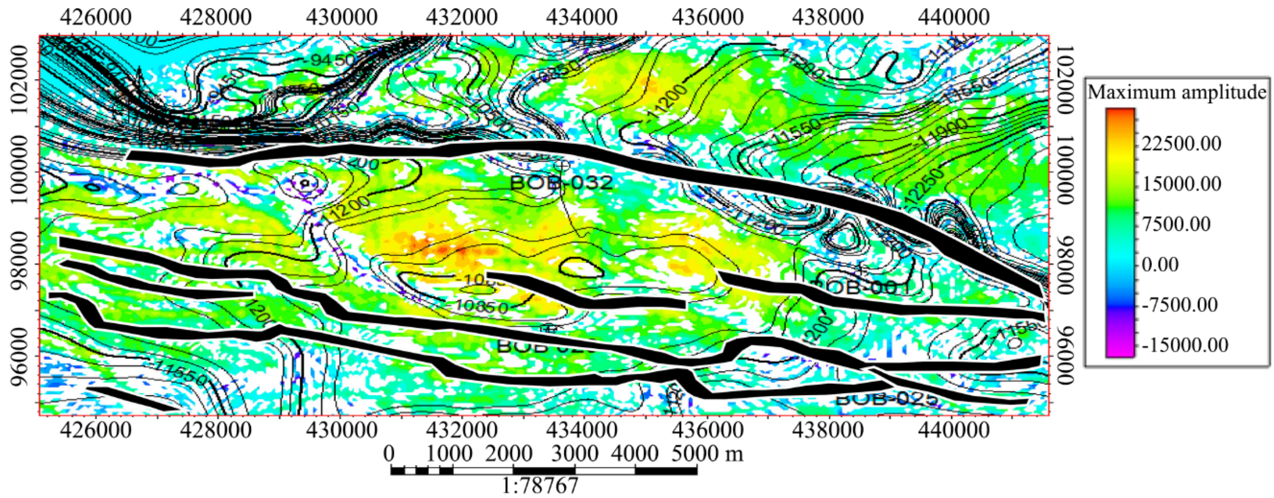

(b)

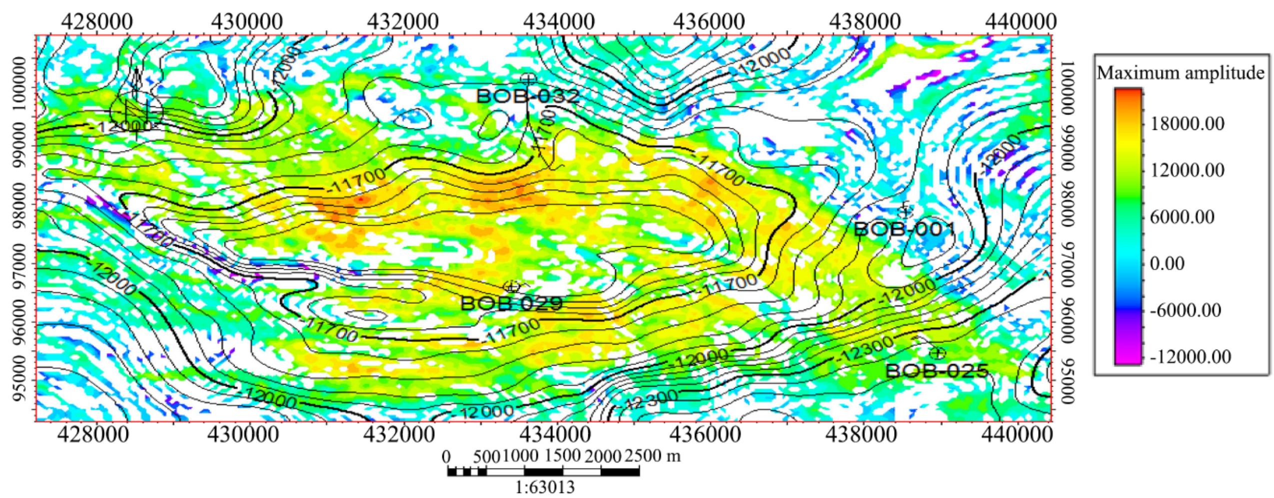

(c)

Figure 10. Maximum amplitude maps extracted from (a) R3 reservoir, (b) R4 reservoir and (c) R5 reservoir showing high amplitude zones (green, yellow and red colours) as areas of potential oil accumulation (brightspots) areas (generated by the authors during this study).

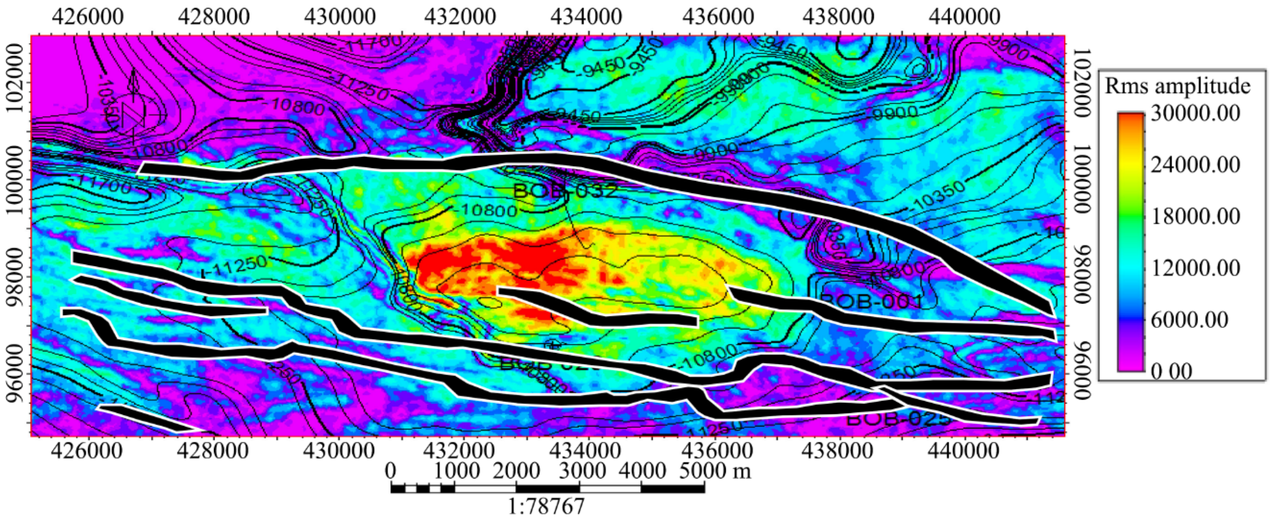

(a)

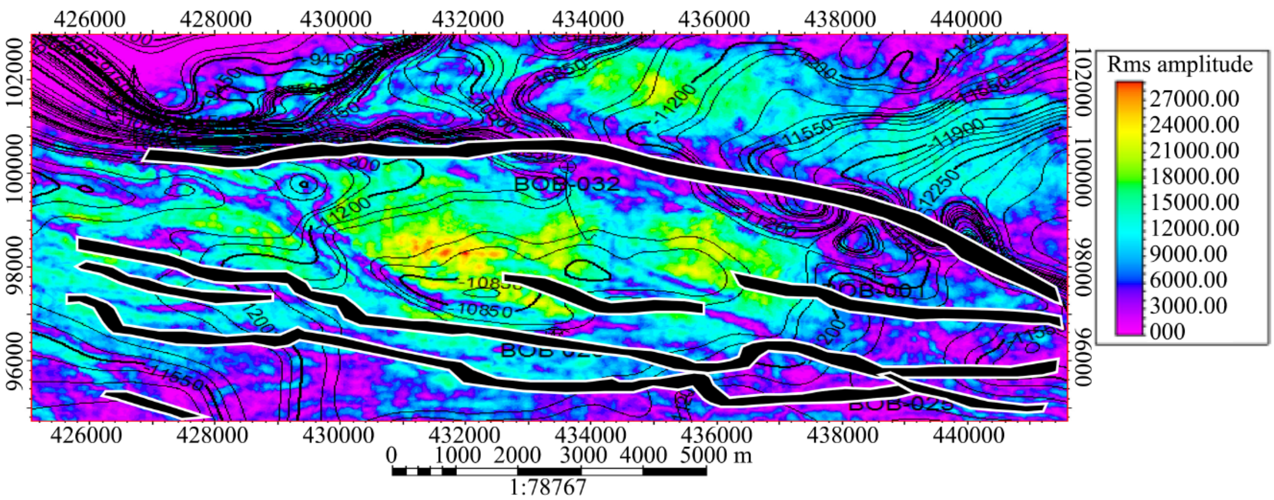

(b)

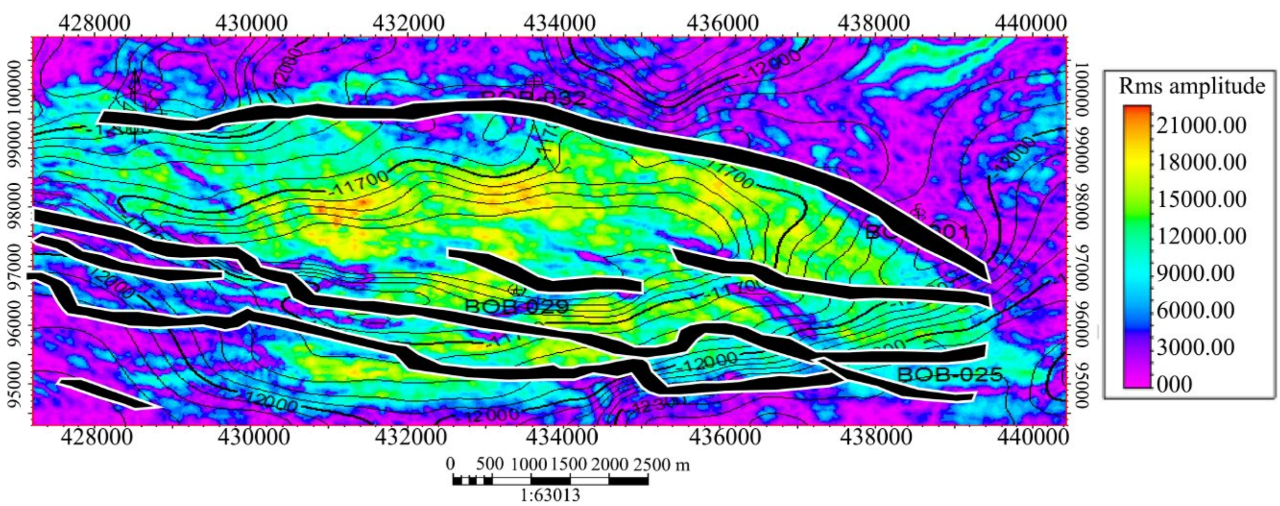

(c)

Figure 11. RMS amplitude maps of (a) R3 reservoir, (b) R4 reservoir and (c) R5 reservoir showing high amplitude zones (red, yellow and green) which is possible hydrocarbon accumulation (bright spots) areas (generated by the authors during this study).

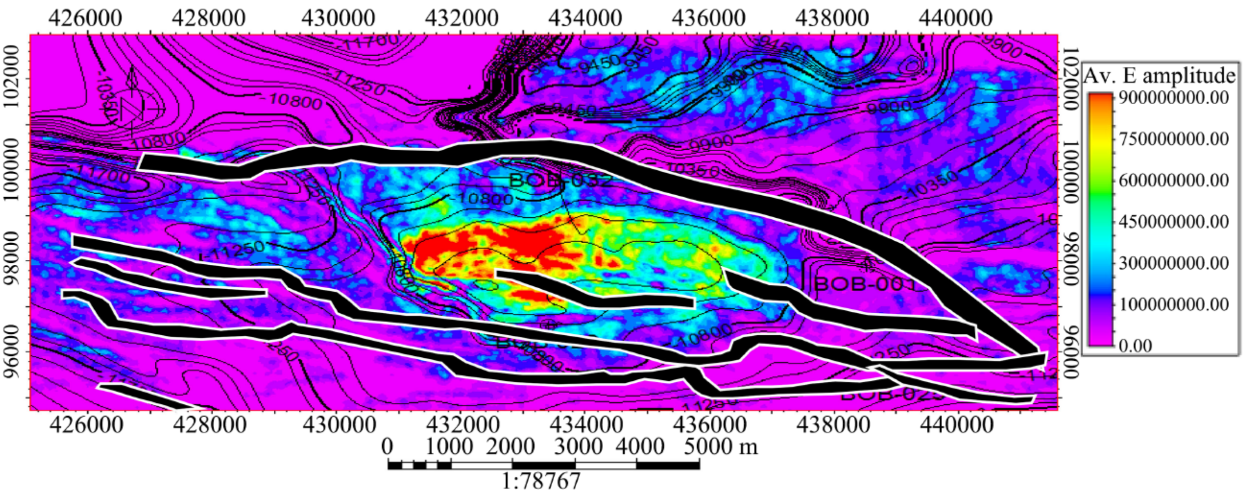

(a)

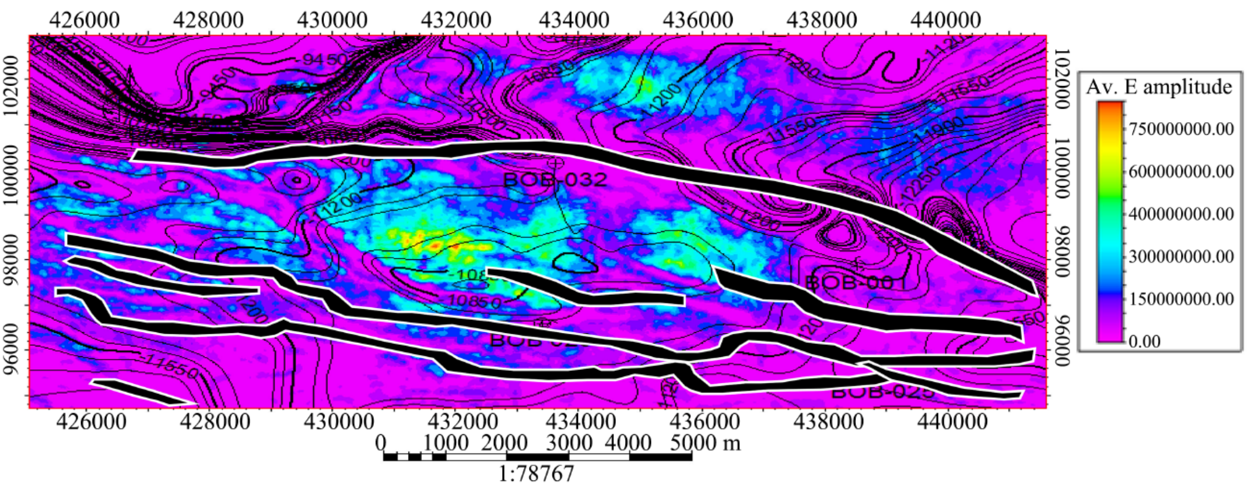

(b)

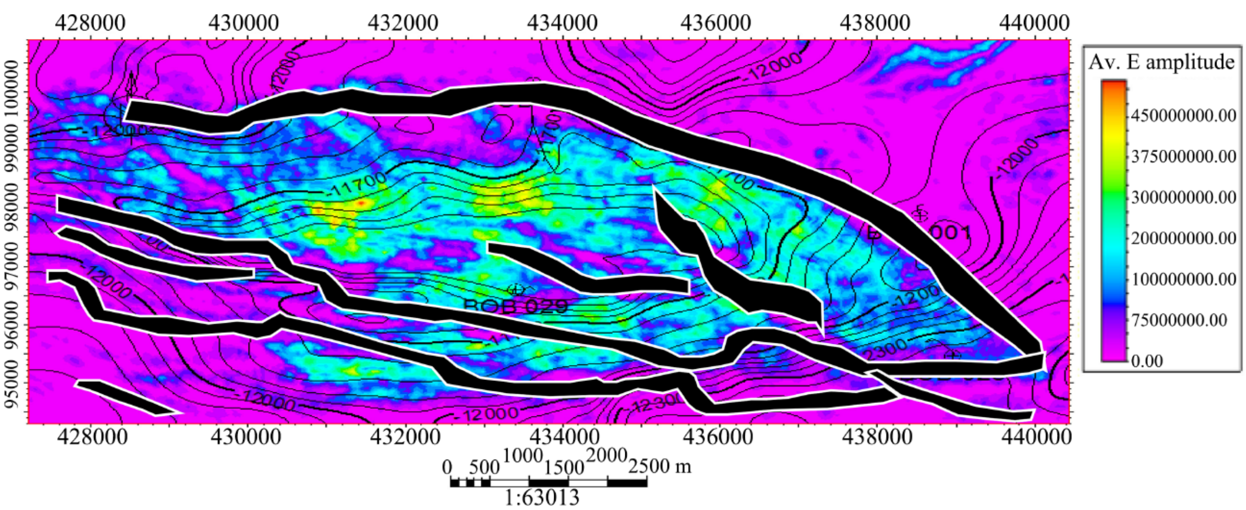

(c)

Figure 12. Average energy extraction maps of (a) R3 reservoir, (b) R4 reservoir and (c) R5 reservoir showing high amplitude zones (red, yellow and green) which is possible hydrocarbon accumulation (bright spots) areas (generated by the authors during this study).

excellent consistency in the anomaly for each of these properties in identifying the prospects over the 3 reservoirs. Since the R3, R4 and R5 mark the top of each reservoir, the high amplitude recorded on the horizon indicates the presence of hydrocarbon within the mapped reservoir. This supports the results of the well-log analysis. Each of the amplitude anomalies is structurally controlled. Of these, the maximum amplitude anomaly map has been used for the prospectivity analysis.

4.3.1. Maximum Amplitude Analysis

Maximum amplitude extraction was performed on the mapped 3 reservoir surfaces to correctly establish the relationship between the observed lithology and the seismic loop. The result of the amplitude extraction on R3, R4 and R5 reservoir sand shows relatively high amplitude zone **limited to three colors (purple, yellow and brown)** which ranges from 6000 - 33,000 for R3 reservoir, 15,000 - 30,000 for R4 reservoir and 6000 - 22,000 for R5 reservoir. At the northwest, south east, the high amplitude zones (brown and yellow) represents hydrocarbon saturated sand units. **The brown and** yellow coloured areas represent highly porous formation with hydrocarbon prospect. The purple and blue zones are porous unit with brine. The brown/black areas concentrated at the steep contours coincide with the location of the faults (compare **Figures 10-12**). Bright spots tend to increase from the northwest to the south east and north east. The high amplitude lobe implies considerable hydrocarbon saturation. The existing wells tap from the oil pool with the highest amplitude anomaly (red coour).

The prospects are compartmentalized by the prevailing fault system and are hence structurally conttroled as each prospect is bound by separate anticline as seen from the contours. There is evidence of low maximum amplitudes (pink and blue colour) at the boundary of each prospect which coincide with the faults (see **Figures 10-12**).

4.3.2. Root Mean Square Amplitude Analysis

The RMS amplitude map of the horizons show high amplitude zones limited to three major colours (green, yellow and red) with ranges from 18,000 - 30,000, 18,000 - 27,000 and 15,000 - 21,000 for R3, R4 and R5 reservoirs, respectively. The high amplitude zones (green, yellow and red) represent hydrocarbon saturated sandstone units. The green, yellow and red coloured areas represent highly porous formation with hydrocarbon accummulation. The background purple colour and sky blue is represents zones occupied by brine or unsaturation (**Figure 11**). The puple colour and areas interspersed by the very steep contours indicates zones occupied by the faults with enough baffles to flow of the hydrocarbon. The hence represent the comaprtmentalizing boundaries for each prospect. The high hydrocarbon accummulation at the center of the study area with existing 2 wells show the accummulation bounded by the 10800 ft contour.

4.3.3. Average Energy Amplitude Analysis

Average energy extraction maps of the horizons shows similarity in lateral distribution, and hydrocarbon prospect zones. The average energy amplitude map of the various horizons shows high amplitude zones limited to three major colours (green, yellow and red). They range from 600,000,000 - 900,000,000, 450,000,000 - 750,000,000 and 30,000,000 - 4,500,000,000 for R3, R4 and R5 reservoirs, respectively. Bright spots which are a Direct Hydrocarbon Indicator (DHI) were seen as a result of decrease in impedance of the hydrocarbon saturated and unsaturated or brine saturated sandstone unit. The anomalous amplitudes in form of brightspots (green, yellow and red) observed on the surfaces indicates that the central zone is a sandstone unit, possibly channel fills. This thus becomes the carrier beds conveying the hydrocarbon into the respective traps basinward. The high amplitude areas are concentrated around the structural highs (NW-SE). **Figure 12** shows the average energy amplitude map for the study area.

4.3.4. Prospectivity from Seismic Property Analysis

Amplitude extraction map (maximum amplitude) exposes areas of bright spot across the field. This analysis was carried out for ***each of the three reservoirs*** (R3, R4 and R5). The maximum amplitude map generated aided the prospect delineation based on the bright spot observed (**Figures 13-15**).

4.4. Formation Evaluation Results and Interpretation

Three reservoirs were evaluated (R3, R4 and R5), the results are discussed as follows: The Net-to-Gross (N/G), Volume of Shale (Vs), Water Saturation (Sw), Porosity (POR) are expressed as volume fraction.

R3 reservoir

The reservoir has average porosity and permeability values of 0.23 and 993.67 mD, respectively. These porosity-permeability values confirm that the sand has good to very good reservoir quality. The reservoir has an average hydrocarbon saturation of 0.92. The net to gross thickness of the sand increases and decreases eastwards. The petrophysical parameters measured from the reservoir R3 from the 3 wells are shown in **Table 1** and **Figure 16**.

R4 reservoir

The petrophysical evaluation of reservoir R4 shows good average porosity-permeability. The porosity and permeability values of R4 reservoir are 0.22 and

Table 1. Petrophysical parameters for reservoir R3.

WELL	TOP (ft)	BASE (ft)	GROSS THICKNESS (ft)	NET THICKNESS (ft)	N/G THICKNESS	POR (v/v)	Vsh (v/v)	Sw (v/v)	Sh (v/v)	K (mD)
BOB-001	11,494	11,520	26.00	19.00	0.73	0.16	0.22	0.16	0.84	1456.88
BOB-029	11,813	11,831	18.00	16.75	0.93	0.38	0.16	0.01	0.99	975.40
BOB-025	11,872	11,899	27.00	21.75	0.80	0.15	0.06	0.06	0.94	554.74
AVG	-	-	23.66	19.16	0.82	0.23	0.14	0.07	0.92	993.67

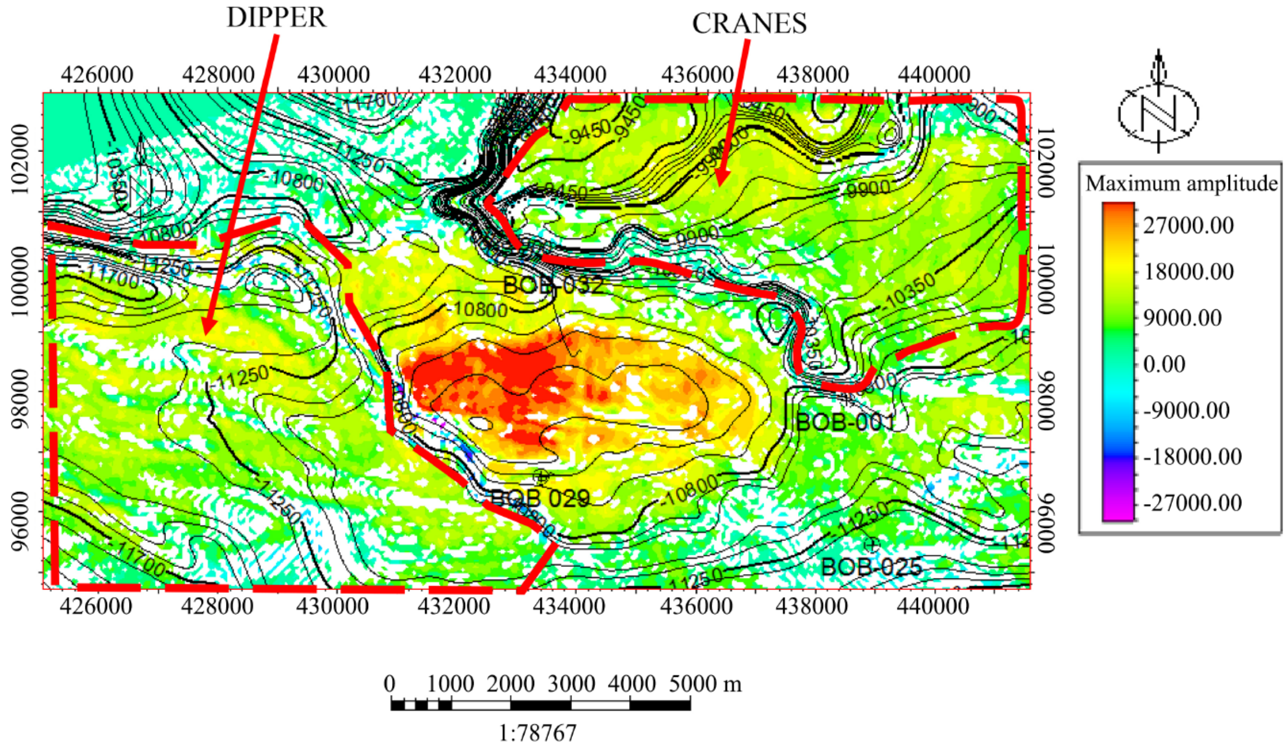

(a)

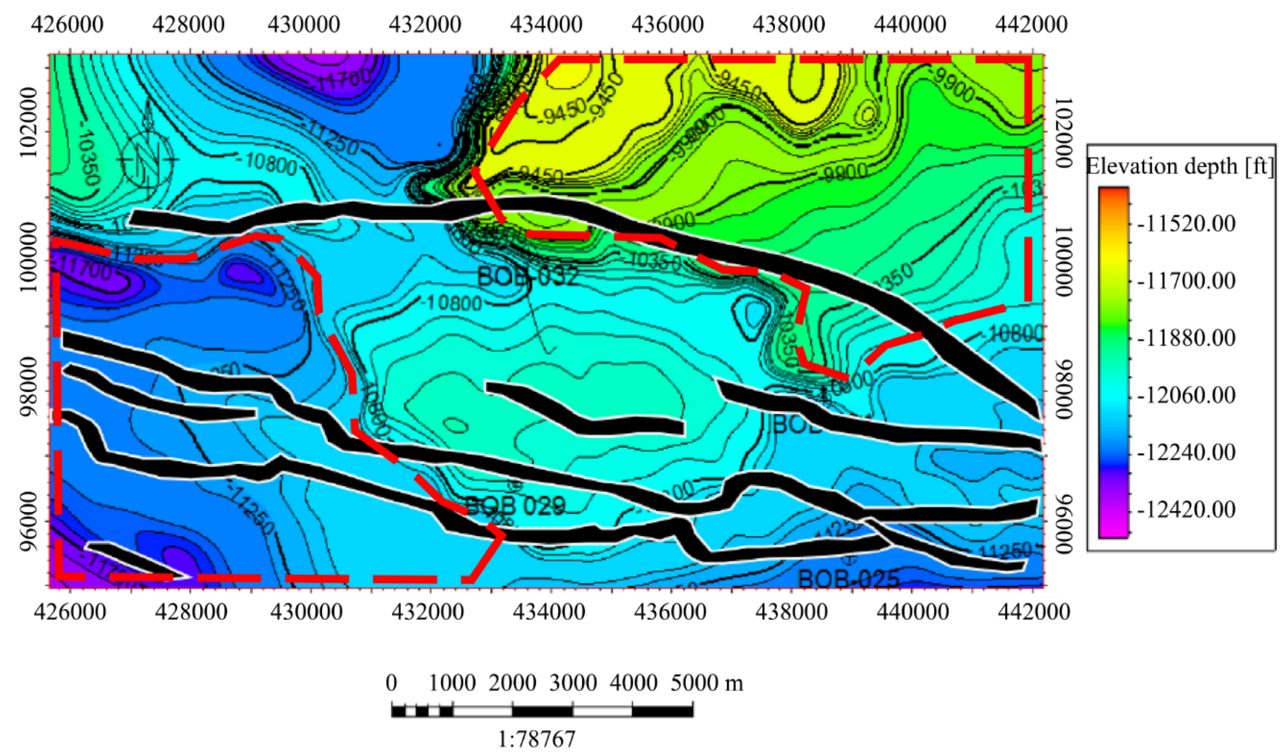

(b)

Figure 13. Maximum amplitude map of (a) R3 reservoir and (b) depth structural map showing the delineated prospect in R3 reservoir (as generated by the authors during this study).

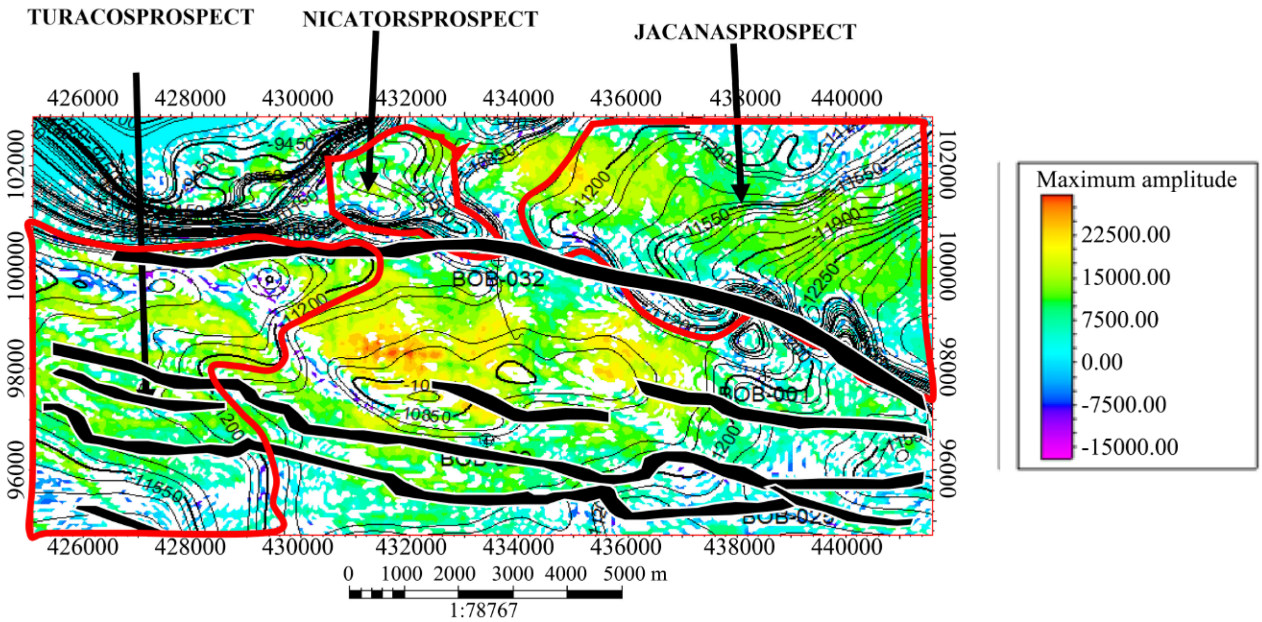

(a)

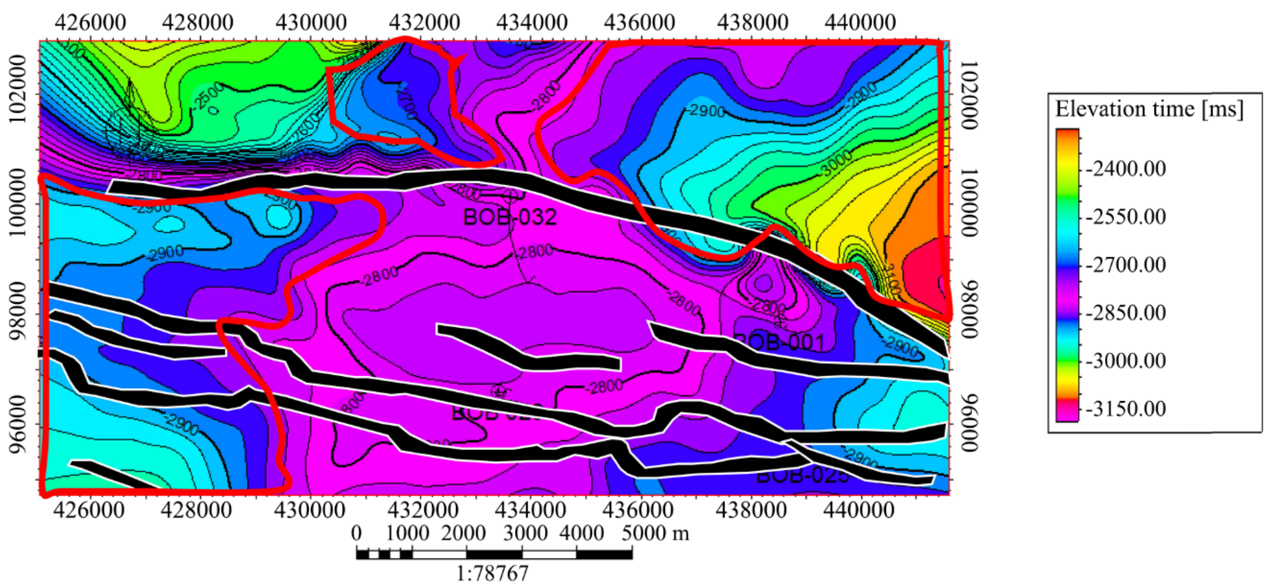

(b)

Figure 14. Maximum amplitude map of (a) R4 reservoir, (b) depth structural map showing the delineated prospect in R4 reservoir (generated by the authors during this study).

1882.39 mD, respectively. Net to gross and volume of shale are 0.91 and 0.13 with hydrocarbon saturation of 0.92. The porosity-permeability values confirm that the sand has good to excellent reservoir quality. Net to gross thickness decreases eastwards. The petrophysical parameters measured from the reservoir R4 from the 3 wells are shown in Table 2 and Figure 17.

R5 reservoir

The "R5" reservoir shows good petrophysical properties with porosity and permeability values of 0.21 and 158.96 mD, and hydrocarbon saturation of 0.88,

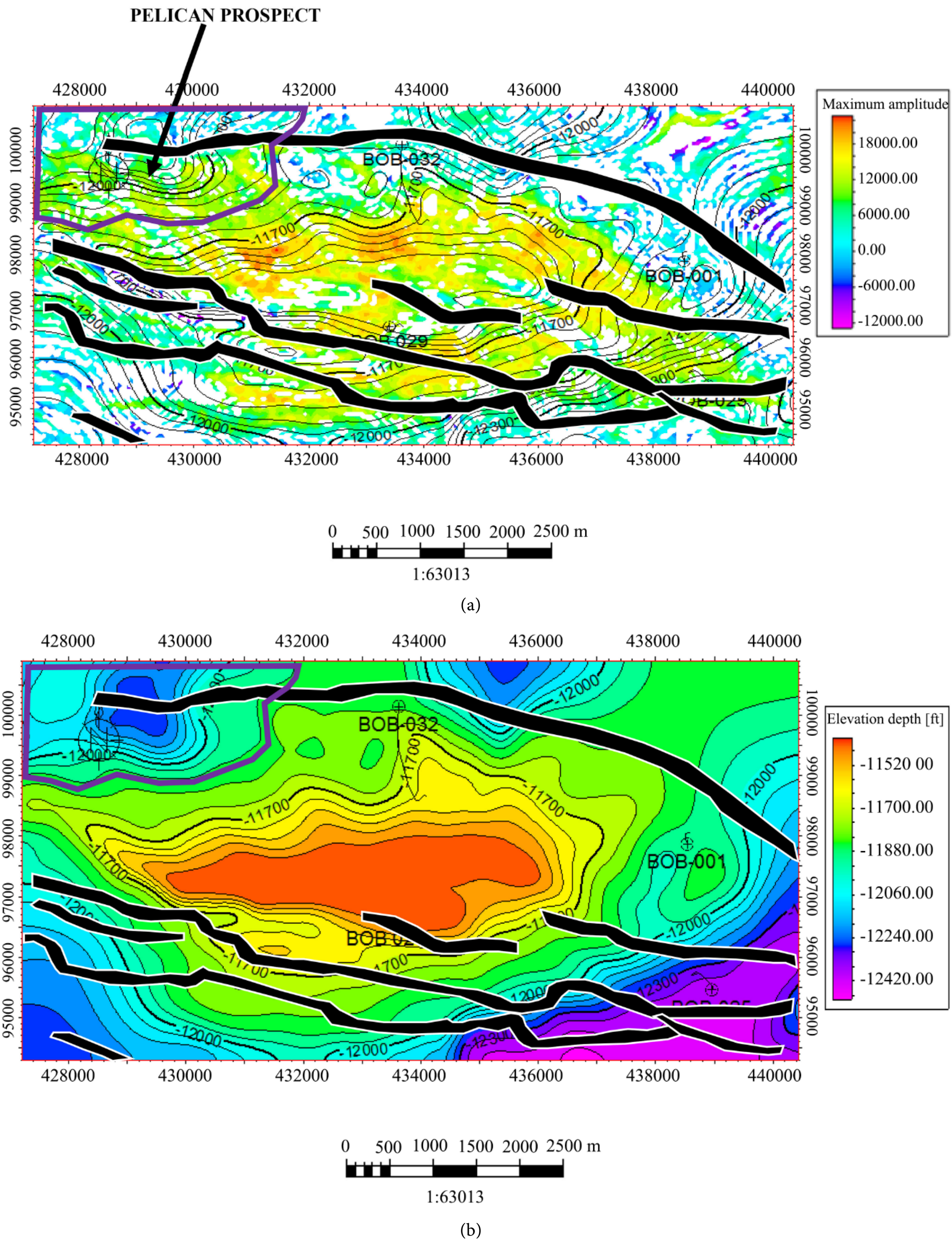

Figure 15. Maximum amplitude map of (a) R5 reservoir, (b) depth structural map showing the delineated prospect in R5 reservoir (generated by the authors during this study).

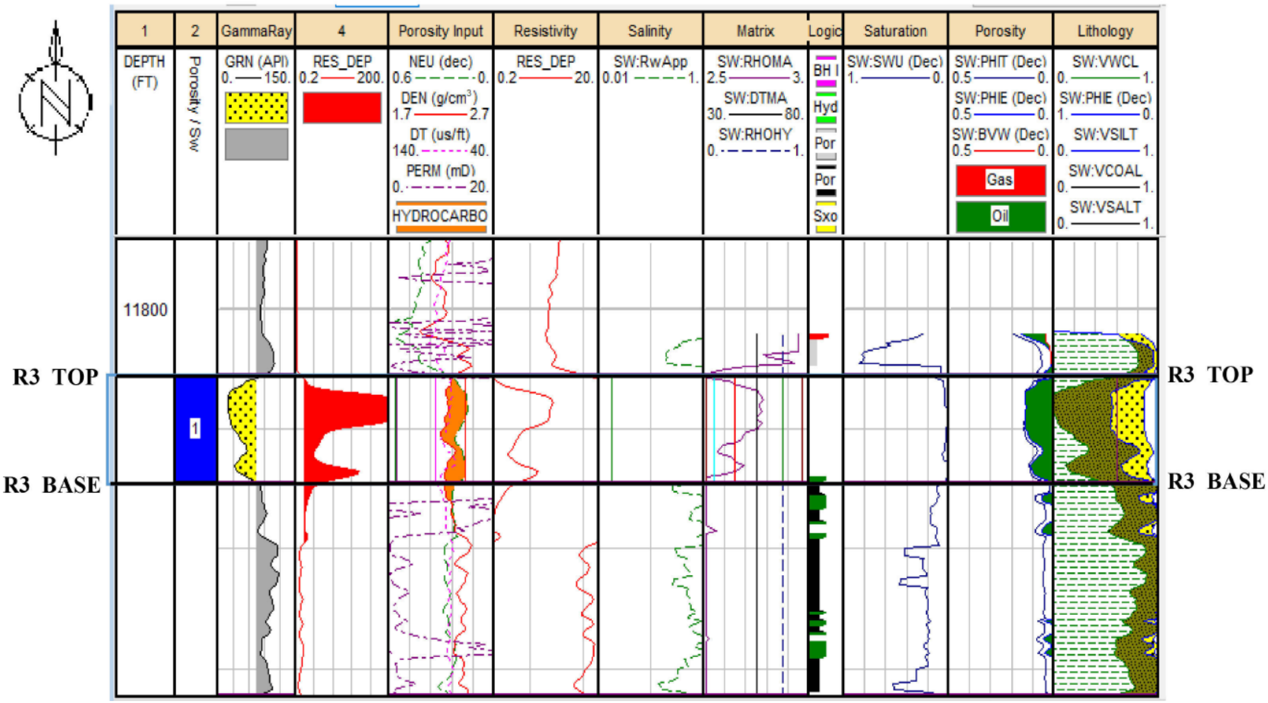

Figure 16. Correlation panel across the field showing log-derived petrophysical properties of reservoir R5 (with the interval, top and base, highlighted in blue colour zone 1). The log-derived data follow computed average petrophysical parameters from the well log from the 3 wells (Bob-001, Bob-025 & Bob-029), all of which cut across each referenced reservoir.

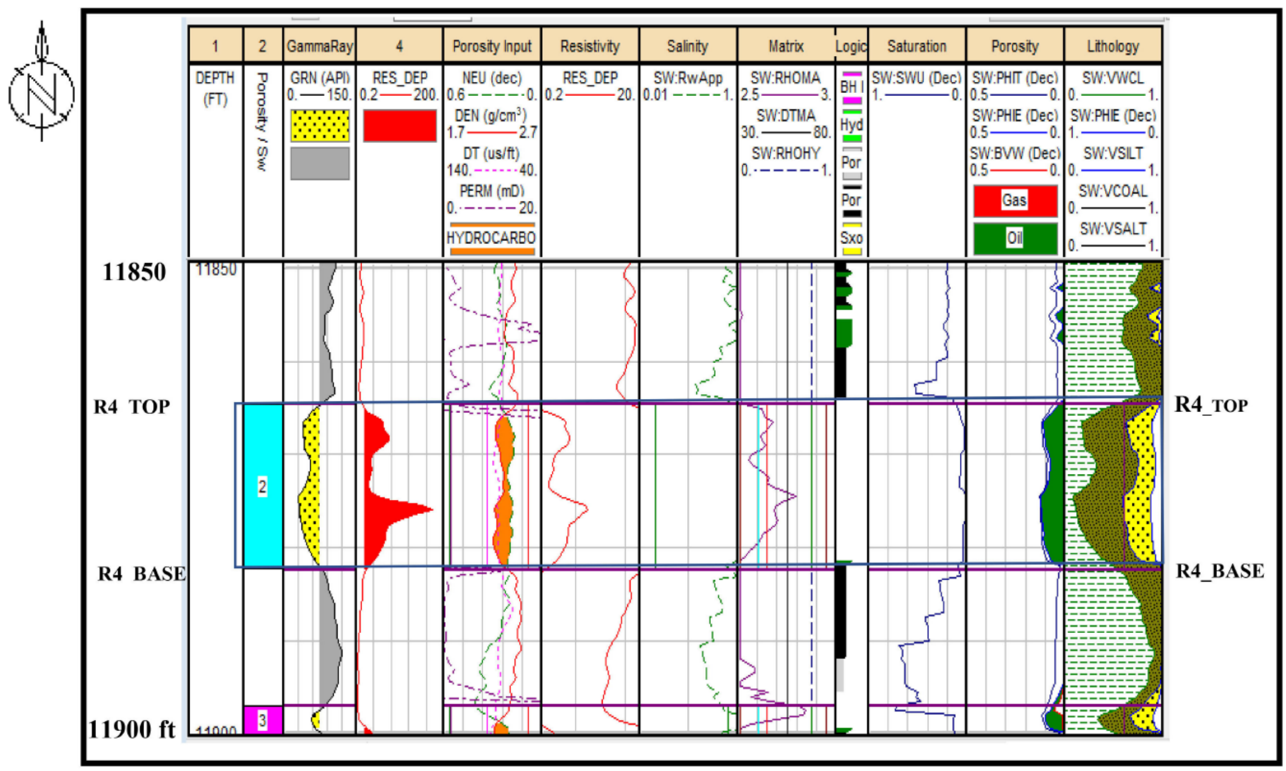

Figure 17. Correlation panel across the field showing log-derived petrophysical properties of reservoir R5 (with the interval, top and base, highlighted in light green colour zone 2). The log-derived data follow computed average petrophysical parameters from the well log from the 3 wells (Bob-001, Bob-025 & Bob-029), all of which cut across each referenced reservoir.

Table 2. Petrophysical parameters for reservoir R4.

WELL	TOP (ft)	BASE (ft)	GROSS THICKNESS (ft)	NET THICKNESS (ft)	N/G THICKNESS	POR (v/v)	Vsh (v/v)	Sw (v/v)	Sh (v/v)	K (mD)
BOB-001	11,531	11,674	143	109.60	0.76	0.15	0.12	0.18	0.82	2632.97
BOB-029	11,866	11,883	17.00	16.75	0.98	0.34	0.23	0.02	0.98	973.2
BOB-025	11,934	11,940	6.00	5.80	0.96	0.17	0.05	0.04	0.96	2041.01
AVG	-	-	55.33	44.05	0.90	0.22	0.13	0.08	0.92	1882.39

respectively, which shows that the reservoir holds a significant volume of hydrocarbons for production. These porosity-permeability values confirm that the sand has good to very good reservoir quality. There is a dynamic change in the net to gross thickness of the sand down dip. The petrophysical parameters measured from the reservoir R5 from the 3 wells are shown in **Table 3** and **Figure 18**.

4.5. Volumetric Analysis

From the study, the reservoirs R3, R4 and R5 studied are saturated by oil, hence the volume estimation was based on the computation of the stock tank oil initially in place using the formula shown in Equation (8). This was carried out using the Petrel software and the petrophysical parameters in **Tables 1-3** that were interpreted for the prospects in the reservoirs, R3, R4 and R5, respectively. Petrophysical parameters were computed for the reservoirs from the logs, using the Interective Petrophysics (IP) software. These parameters estiamtes the total area and volume space of the delineated prospects for this computation.

Using the IP software, the GROSS rock volume, net to gross, porosity, water (and hence hydrocarbon) saturation, were estiamted. Available production data, relating to the formation volume factor, was employed for the volumetric estimation. The volume estimated for the delineated prospects in Reservoir, R3 is 12.73 and 6.84, Million barrels of oil (Mbls) for Dipper and Crane prospects, respectively. The prospects in reservoir, R4, yielded 11.32, 8.62, and 7.42 Million barrels (Mbls) for Turacos, Nicators and Jacana, respectively, while the lone prospect in reservoir R5 (Pelicans), was estimated at 4.76 Million barrels of oil (**Table 4**).

4.6. Play Risk Analysis

The subsurface data shows that wells "Bob"-001, "Bob"-029 and "Bob"-025 cut into the shales of Agbada Formation. The hydrocarbon bearing reservoirs was penetrated by wells "Bob"-001, "Bob"-029 and "Bob"-025. The reservoir sand varies in thickness and is evenly distributed across the above listed wells. The seal rock within the study area is the laterally extensive Shales of Agbada Formation. There is a good lateral distribution of the top seals penetrated by the

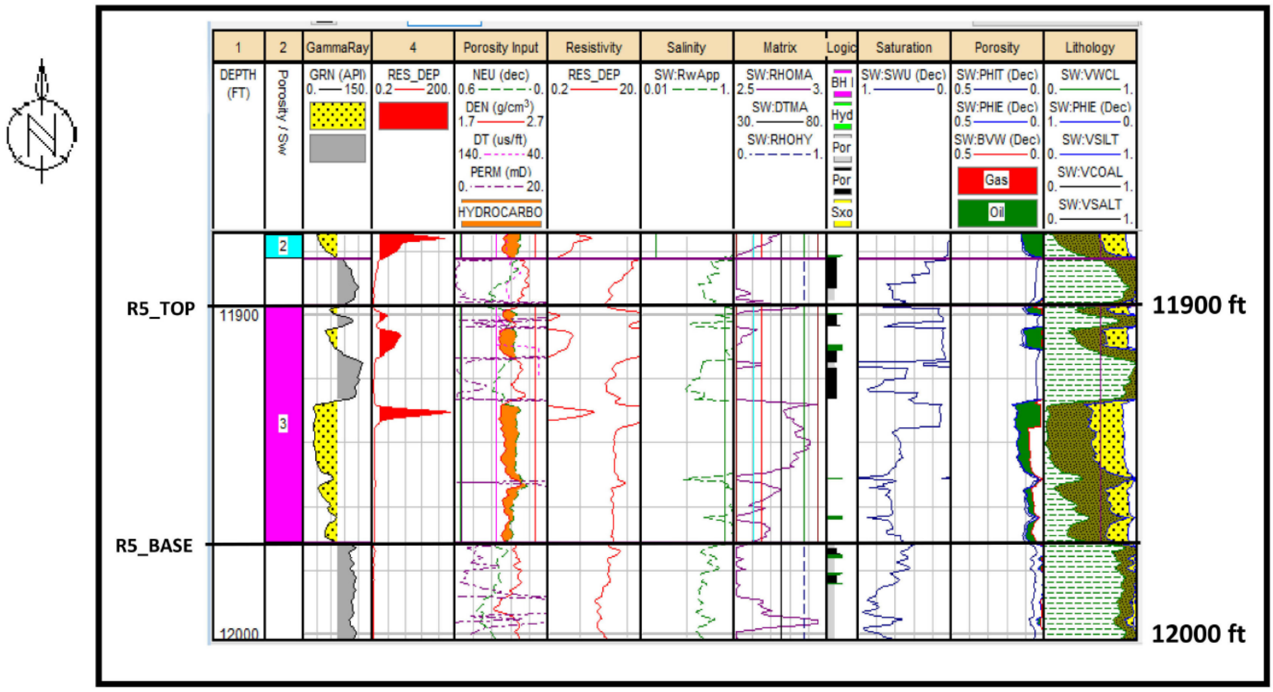

Figure 18. Correlation panel across the field showing log-derived petrophysical properties of reservoir R5 (with the interval, top and base, highlighted in purple colour zone 3). The log-derived data follow computed average petrophysical parameters from the well log from the 3 wells (Bob-001, Bob-025 & Bob-029), all of which cut across each referenced reservoir.

Table 3. Petrophysical parameters for reservoir R5.

WELL	TOP (ft)	BASE (ft)	GROSS THICKNESS (ft)	NET THICKNESS (ft)	N/G THICKNESS	POR (v/v)	Vsh (v/v)	Sw (v/v)	Sh (v/v)	K (mD)
BOB-001	**11,687**	**11,692**	**5.00**	**4.20**	**0.84**	**0.21**	**0.14**	**0.13**	**0.87**	304.56
BOB-029	**11,896**	**11,971**	**75.00**	**53.75**	**0.71**	**0.35**	**0.21**	**0.06**	**0.94**	97.00
BOB-025	**11,861**	**11,900**	**39.00**	**31.00**	**0.79**	**0.18**	**0.10**	**0.16**	**0.84**	75.34
AVG	-	-	39.66	29.65	0.78	0.21	0.15	0.11	0.88	158.96

Table 4. Volumetric analysis showing the quantity of hydrocarbon in R3, R4 and R5 reservoirs.

RESERVOIR	PROSPECTS	AVG NET TO GROSS (N/G)	AVG POROSITY	AVG HYDRO-CARBON SATURATION (SHC)	FORMATION VOLUME FACTOR (FVF)	GROSS ROCK VOLUME (FT^3)	STOIIP (Bbls)
R3	DIPPERS	0.82	0.23	0.92	1.29	946394489095.52	12.73
	CRANES	0.82	0.23	0.92	1.29	508999310177.75	6.84
R4	TURACOS	0.90	0.22	0.92	1.29	801781513462.27	11.32
	NICATORS	0.90	0.22	0.92	1.29	610177133594.66	8.62
	JACANAS	0.90	0.22	0.92	1.29	525594697386.99	7.42
R5	PELICANS	0.78	0.21	0.88	1.29	42559469738.99	4.76

wells. The play risk analysis of the study area was carried out through the generation of the thickness map from the seal, reservoir distribution map from the

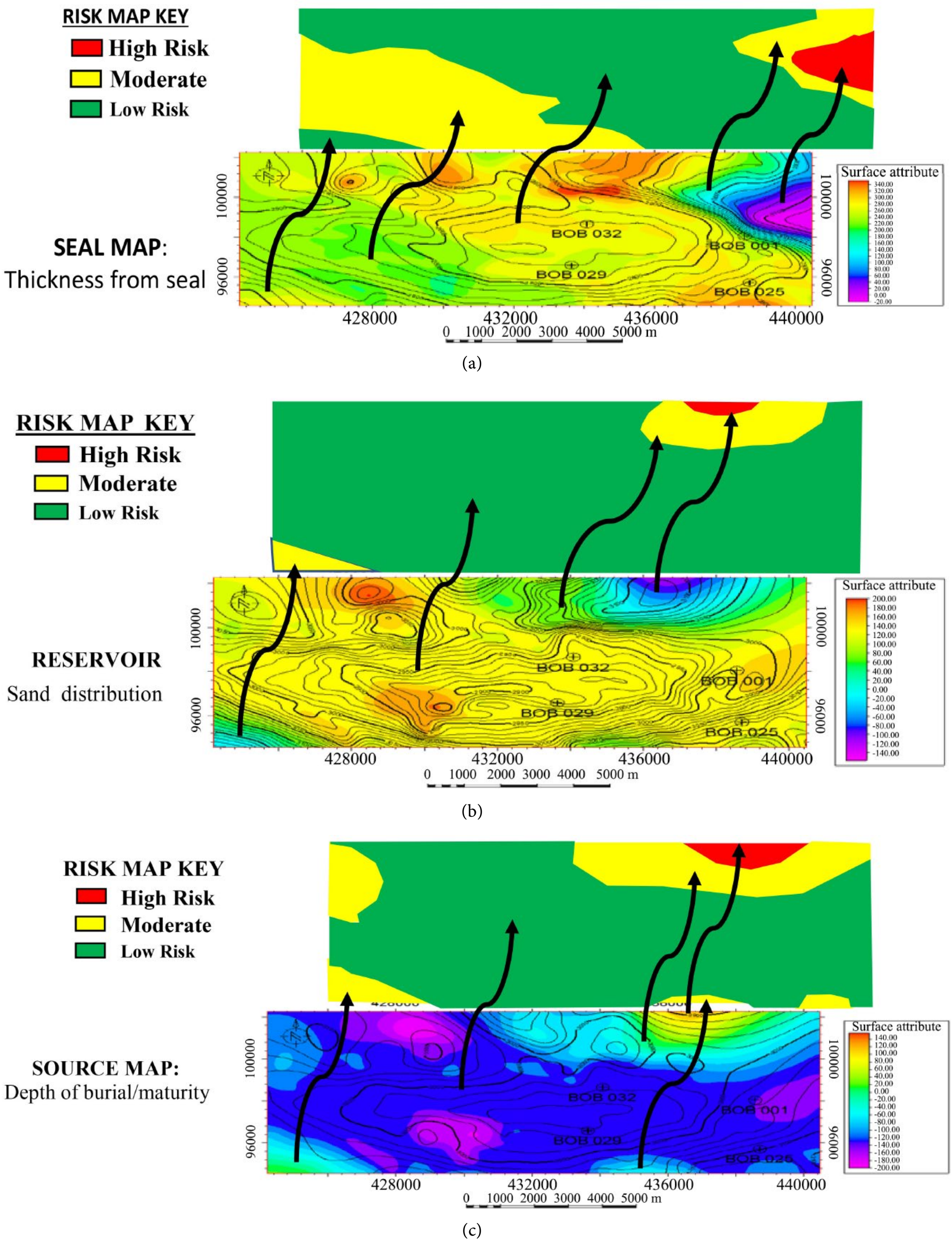

Figure 19. Play risk maps generated from each of (a) seal thickness, (b) sandstone (reservoir) distribution and (c) source thickness map within the study area. Arrows point from respective maps zones to the equivalent risk map as rated in the interpretation.

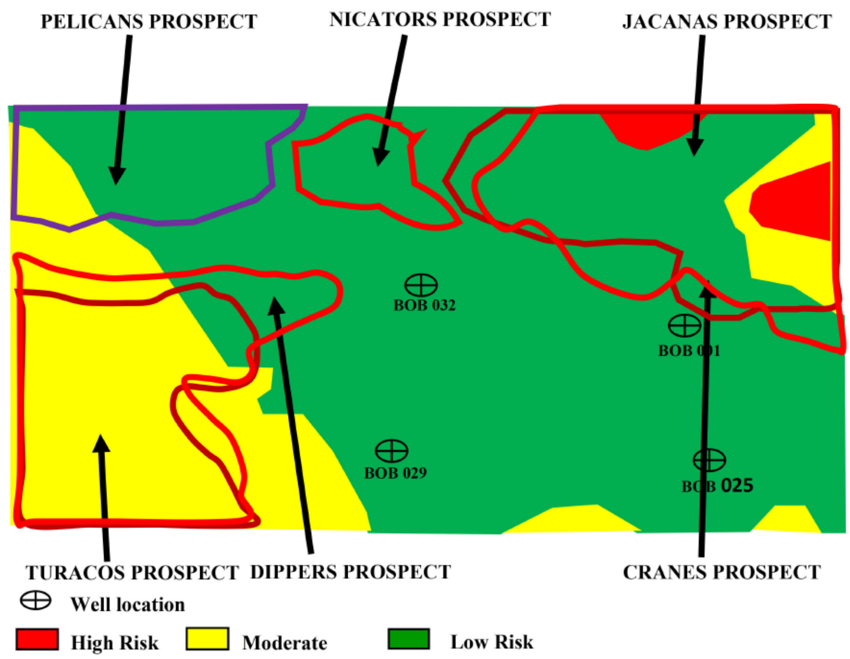

Figure 20. Composite Risk Segment (CRS) map of the petroleum play in the study area showing the delineated prospects.

reservoir and depth of burial map from the source. Figure 19 shows the Play risk maps generated from each of (a) seal thickness, (b) sandstone (reservoir) distribution and (c) source thickness map within the study area. The risk maps are placed above each of the seal, reservoir and source maps, respectively with arrows pointing from these maps to the equivalent risk map zones as interpreted. The result of the playrisk analysis shows that the area has good source/seal tickness and reservoir which tallies with the delineated prospect located within the low-risk area. The green coloration seen in the play risk map is the identified low-risk area. The yellow shade was denoted as areas with moderate risk, while the red shade shows the areas with high risk within the study area. The presence of a well-delineated low-risk portion suggests a favorable hydrocarbon exploration target. Common risk segment maps were developed with descriptions of the various elements from corresponding seismic-derived maps (Figure 20). Composite common risk segment maps were used to identify low-risk areas for exploration. It was established that Turacos, Dippers and Pelicans prospects fell within moderate to low risk, Nicators prospects fell specifically within the low-risk area while Jacanas and Cranes prospects span through low, moderate to high risk.

5. Conclusions

Three reservoirs are identified, namely reservoirs R3, R4, and R5, and are correlatable across the field with shaliness increasing with depth. The structures present include listric faults (antithetic and synthetic), and a regional fault. The faults and reservoir architecture support the accumulation and entrapment of hydrocarbon in the 3 reservoirs. All 3 types of amplitude maps generated, namely maximum amplitude, root mean square and average energy generated yielded 6 identifiable prospects in the study area. From the maximum amplitude map, the booming amplitude zones are conformable to the structures present. The petrophysical parameters for each reservoir are: for porosity: 0.23, 0.22 and 0.21, respectively; for permeability: 993.67, 1882.39 and 158.96 mD, respectively and for water saturation: 0.07, 0.08 and 0.11, respectively.

The volumes estimated for the delineated prospects in reservoir R3 are 12.73 and 6.84, Million barrels (Mbls) of oil for Dipper and Crane prospects, respectively. The prospects in reservoir R4, yielded 11.32, 8.62, and 7.42 Million barrels (Mbls) of oil for Turacos, Nicators and Jacana, respectively, while the only 1 prospect in reservoir R5 (Pelicans) was estimated at 4.76 Million barrels of oil. This represents a total volume of 51.69 (Mbls) over a column of 66 ft reservoir sand in the study area.

Play risk studies yielded recognizable distinct play risk isochron maps from the reservoir and seal/trap data classified as low, moderate and high-risk zones based on the reservoir and source/trap distribution in the study area. While reservoirs R3 and R4 have variable low, moderate to high-risk zones, R5 is located within low to moderate risk. Of the 6 prospects, the Pelicans' and Nicators' prospects have the lowest risk with a high volume of oil; Turacos' and Dippers' prospects have moderate risk while Jacanas' and Cranes' prospects have the highest risk with minimal promise for good oil accumulation. Therefore, the reservoir showed good structural control with a good amount of hydrocarbon accumulations and measurable degrees of risk factors capable of narrowing the hydrocarbon risk and enhancing management decisions in the choice of drilling in the identified prospects.

Acknowledgements

We wish to extend our profound gratitude to the Shell Petroleum Development Company (SPDC) of Nigeria for always supporting the Department of Geology with datasets for academic research through the Department of Petroleum Resources, Port Harcourt, Nigeria, who approved the release of the data for research.

Funding

The authors affirm that there is no grant in support of this study

Availability of Data and Material

Data is usually released by Shell Petroleum Development Company through the Department of Petroleum Resources to assist research in universities in Nigeria.

Code Availability

Industry-university support suite of software in the Department of Geology, University of Nigeria.

Conflicts of Interest

The authors declare that they have no conflict of interest.

References

[1] Wiener, R.W., Helwig, J.A. and Rongpei, J. (1997) Seismic Interpretation and Structural Analysis of a Rifted Thrust Belt: Jianghan Basin, China. *The Leading Edge*, **16**, 1177-1183. https://doi.org/10.1190/1.1437762

[2] El-Mowafy, H. and Marfurt, K.J. (2008) Structural Interpretation of the Middle Frio Formation Using 3D Seismic and Well Logs: An Example from the Texas Gulf Coast of the United States. *The Leading Edge*, **27**, 840-854. https://doi.org/10.1190/1.2954023

[3] Opara, A.I. (2010) Prospectivity Evaluation of "USSO" field, Onshore Niger Delta Basin, Using 3-D Seismic and Well Log Data. *Petroleum & Coal*, **52**, 307-315.

[4] Opara, A.I., Anyiam, U.O. and Nduka, A.V. (2011) 3-D Seismic Interpretation and Structural Analysis of Ossu Oil Field, Northern Depobelt, Onshore Niger Delta, Nigeria. *The Pacific Journal of Science and Technology*, **12**, 502-509.

[5] Anyiam, O.A., Maduewesi, C.O., Ibemesi, P.O. and Okwara, C.O. (2017) Reservoir Quality Studies and Prospect Identification of a Field in Coastal Swamp Depobelt. *Petroleum and Coal*, **59**, 505-515.

[6] Oyeyemi, K.D., Olowokere, M.T. and Aizebeokhai, P. (2018) Hydrocarbon Resource Evaluation Using Combined Petrophysical Analysis and Seismically Derived Reservoir Characterization, Offshore Niger Delta. *Journal of Petroleum Exploration and Production Technology*, **8**, 99-115. https://doi.org/10.1007/s13202-017-0391-6

[7] Mode, A.W. and Anyiam, A.O. (2007) Reservoir Characterization: Implications from Petrophysical Data of the "Paradise-Field", Niger Delta, Nigeria. *Pacific Journal of Science and Technology*, **8**, 194-202.

[8] John, O.A. and Oluwaseyi, A.O. (2013) Petrophysical Properties Evaluation for Reservoir Characterisation of SEYI Oil Field (Niger-Delta). *International Journal of Innovation and Applied Studies*, **3**, 765-773.

[9] Kulke, H. (1995) Nigeria. In: Kulke, H., Ed., *Regional Petroleum Geology of the World. Part II: Africa, America, Australia and Antarctica*, Gebruder Borntraeger, Berlin, 143-172.

[10] Kaplan, A., Lusser, C.U. and Norton, I.O. (1994) Tectonic Map of the World, Panel 10. *American Association of Petroleum Geologists Bulletin*, **60**, 230-237.

[11] Ekweozor, C.M. and Daukoru, E.M. (1994) Northern Delta Depobelt Portion of the Akata-Agbada(!) Petroleum System, Niger Delta, Nigeria. In: Magoon, L.B. and Dow, W.G., Eds., *The Petroleum System—From Source to Trap*, Vol. 60, American Association of Petroleum Geologists, 599-599. https://doi.org/10.1306/M60585C36

[12] Tuttle, M.L.W., Brownfield, M.E. and Charpentier, R.R. (1999) Tertiary Niger Delta (Akata-Agbada) Petroleum System, Niger Delta Province, Cameroon and Equatorial Guinea, Africa. U.S Geological Survey Open File Report, 1-13.

[13] Doust, H. and Omatsola, E. (1990) Niger Delta. In: Edwards, J.D. and Santogrossi, P.A., Eds., *Divergent/Passive Margin Basins*, Vol. 48, American Association of Petroleum Geologists, 201-238. https://doi.org/10.1306/M48508C4

[14] Ejedawe, J.E., Coker, S.J.L., Lambert-Aikhionbare, D.O., Alofe, K.B. and Adoh, F.O.

(1984) Evolution of Oil-Generative Window and Oil and Gas Occurrence in Tertiary Niger Delta Basin. *AAPG Bulletin*, **68**, 1744-1751. https://doi.org/10.1306/AD46198F-16F7-11D7-8645000102C1865D

[15] Avbovbo, A.A. (1978) Tertiary Lithostratigraphy of Niger Delta: GEOLOGIC NOTES. *AAPG Bulletin*, **62**, 295-300. https://doi.org/10.1306/C1EA482E-16C9-11D7-8645000102C1865D

[16] Dim, C.I.P. (2017) Geologic Framework. In: *Hydrocarbon Prospectivity in the Eastern Coastal Swamp Depo-Belt of the Niger Delta Basin*, Springer, Cham, 9-16. https://doi.org/10.1007/978-3-319-44627-1_2

[17] Corredor, F., Shaw, J.H. and Bilotti, F. (2005) Structural Styles in the Deep-Water Fold and Thrust Belts of the Niger Delta. *AAPG Bulletin*, **89**, 753-780. https://doi.org/10.1306/02170504074

[18] Wyllie, M.R.J., Gregory A.R. and Gardner L.W. (1956) Elastic Wave Velocities in Heterogeneous and Porous Media. *Geophysics*, **21**, 41-70. https://doi.org/10.1190/1.1438217

[19] Timur, A. (1968) An Investigation of Permeability, Porosity, & Residual Water Saturation Relationships for Sandstone Reservoirs. *The Log Analyst*, **9**, Paper No. SPWLA-1968-vIXn4a2.